═══REVIEW COMMONS MANUSCRIPT═══

IMPORTANT:

- Manuscripts submitted to Review Commons are peer reviewed in a journal-agnostic way.
- Upon transfer of the peer reviewed preprint to a journal, the referee reports will be available in full to the handling editor.
- The identity of the referees will NOT be communicated to the authors unless the reviewers choose to sign their report.
- The identity of the referee will be confidentially disclosed to any affiliate journals to which the manuscript is transferred.

GUIDELINES:

- For reviewers: https://www.reviewcommons.org/reviewers
- For authors: https://www.reviewcommons.org/authors

CONTACT:

The Review Commons office can be contacted directly at: office@reviewcommons.org

Molecular basis for the activation of Aurora A and Plk1 kinases during mitotic entry

Pillan A[1,2], Ormancey P[1,2], Ben Choug C[3], Orlicky S[4], Tavernier N[1,2], Van Hove L[1,2], Ossareh-Nazari B[1,2], Joly N[1,2], Sicheri F[4], Lorca T[3] and Pintard L[1,2]

[1] Université Paris cité, CNRS, Institut Jacques Monod, F-75013 Paris, France

[2] Programme Equipe Labellisée Ligue contre le Cancer

[3] Centre de Recherche de Biologie cellulaire de Montpellier, UMR 5237, Université de Montpellier, CNRS, 1919 Route de Mende, 34293 Montpellier Cedex 5, France

[4] Centre for Systems Biology, Lunenfeld Tanenbaum Research Institute, Sinai Health System, Toronto, ON M5G 1X5, Canada; Department of Molecular Genetics, University of Toronto, Toronto, ON M5S 1A8, Canada; Department of Biochemistry, University of Toronto, Toronto, ON M5S 1A8, Canada

Correspondence: lionel.pintard@ijm.fr

Highlights:

- MITOKINAC: a versatile approach that reconstitutes Bora and AURKA-dependent Plk1 T-loop phosphorylation in *E. coli.*
- AlphaFold 3 structural modeling of the phospho-Bora – AURKA complex tested by MITOKINAC using 39 Bora variants.
- Phospho-Bora wraps around the N-terminal lobe of AURKA to position its essential phospho-Serine 112 in the activation loop of AURKA.
- pBora delivers the AURKA activity to the Plk1 T-loop, which is otherwise impervious to AURKA phosphorylation.

Keywords: Cell division - Mitotic kinases - Plk1 - Aurora A - Bora

Running title: Mechanism of Plk1 activation by the pBora•AURKA complex

Abstract

The evolutionarily conserved, intrinsically disordered protein Bora is critical for initiating the activation of mitotic kinases. Once phosphorylated at Ser112 by Cyclin A-Cdk1 kinase, phospho-(p)Bora activates unphosphorylated Aurora A kinase (AURKA), directing it towards Polo-like kinase 1 (Plk1), thus promoting Cyclin B-Cdk1 activation and mitotic entry. Here, by combining structural modelling and *in vitro* assays, we provide evidence that Bora wraps around the N-terminal lobe of AURKA to position its phospho-Ser112 near AURKA's T-loop, mimicking T-loop phosphorylation. Additionally, Bora transiently interacts with the Alpha C helix of the Plk1 kinase domain through a conserved motif, guiding AURKA activity towards the Plk1 T-loop, which is otherwise impervious to phosphorylation by AURKA. We highlight the importance of this motif for Bora function in vitro and during mitotic entry in Xenopus egg extracts. Our results reveal critical molecular details of mitotic kinase activation, which could lead to the development of pathway-specific inhibitors.

Introduction

During mitotic entry, cells profoundly reorganize their architecture and physiology, which is essential for chromosome segregation [1]. Evolutionarily conserved Serine/Threonine kinases, including Aurora A (AURKA) [2,3], Polo-like kinase 1 (Plk1) [4], and Cyclin A/B-Cdk1, orchestrate this reorganization by phosphorylating numerous substrates [5-9]. Plk1 promotes mitotic entry [10-13], centrosome separation and maturation [14], the dissociation of cohesin from chromosomes [15], chromosome condensation [16], nuclear envelope breakdown [17,18], spindle assembly [19], chromosome alignment, spindle checkpoint signaling [20], and cytokinesis [21,22] (For reviews [8,23-26]), while AURKA regulates mitotic entry [10,27], centrosome separation, maturation, and bipolar spindle assembly [28-30] (For reviews [8,23-26,31,32]. Overexpression and misregulation of these kinases have been linked to oncogenic transformations and cancers with poor prognosis. However, despite their fundamental importance for cell division, the molecular mechanism by which these kinases are activated during mitotic entry is incompletely understood and is the focus of our study.

Like most eukaryotic kinases, mitotic kinases have a similar structure consisting of an N- and a C-terminal lobe connected by a flexible hinge region [33,34]. Located between the two lobes is the activation segment (a.k.a: T-loop), which provides regulatory control in response to phosphorylation by stabilizing the kinase in an active conformation that supports substrate-binding and catalysis [35-38].

Phosphorylation of the T-loop is catalyzed either by autophosphorylation or by a distinct upstream kinase. For Plk1, the T-loop is phosphorylated by AURKA on the Thr210 residue (human Plk1) [10,39-41]. AURKA, by contrast, can autophosphorylate its own T-loop (Thr288 on human AURKA) [42-45], but the site is rapidly dephosphorylated by counteracting phosphatases during the G2 phase of the cell cycle [46-48]. As dephosphorylation maintains AURKA in an inactive state, this raises the crucial question of how AURKA overcomes the repressive effect of phosphatases to drive mitotic commitment.

AURKA activation is controlled by auto-phosphorylation and dephosphorylation of the T-loop by multiple phosphatases. However, full activation also requires binding to one of several allosteric modulators, including Tpx2 (Targeting protein for Xklp2), Cep192 (Centrosomal protein 192), and TACC3 (Transforming Acidic Coiled-Coil Containing Protein 3). Each of these allosteric modulators also localizes AURKA to specific cellular

structures during mitosis, thereby providing an additional level of regulatory control [9,49,50].

One of the best-characterized AURKA activators is the microtubule-binding protein Txp2, which recruits and activates AURKA at microtubules for mitotic spindle assembly [43,51,52]. Tpx2 binds the N-lobe of AURKA via its first 43 amino acids, using two separate linear sequences, the M1 (aa 7–21) and M2 (30-43) motifs [44] (**Fig. 1A, 1B,** right panels). By binding to AURKA, Tpx2 induces conformational changes leading to a fully active conformation of the kinase (**Fig. 1A**, right panel) [44,45,53-55].

The protein Bora (Aurora Borealis) [56] is another allosteric modulator critically required for AURKA activation during mitotic entry (**Fig. 1A**, left panel). In particular, Bora stimulates AURKA phosphorylation of the T-loop of Plk1 (**Fig. 1A**) [10,41,50,57-59]. However, to do so, Bora must first be phosphorylated by the S-G2 Cyclin A-Cdk1 kinase [57,60,61] (**Fig. 1A**). Cyclin A-Cdk1 selectively phosphorylates Bora at 27 serine/threonine sites followed by proline (S/T-P sites), but among these, only the phosphorylated Serine 112 is critically required for AURKA activation. Indeed, a phospho-null mutation of this site prevents timely mitotic entry in Xenopus egg extracts and human cells [60]. Bora phosphorylated at S112 preferentially binds and activates AURKA lacking phosphorylation on its T-loop (as mimicked by a Thr288Val mutation [$AURKA^{T288V}$]) [59]. This observation explains how AURKA, maintained in its inactive dephosphorylated state by phosphatases in the G2 phase of the cell cycle, can be activated during mitotic entry [59]. Our working model is that phospho-Ser112 on Bora physically substitutes *in trans* for the phosphorylated T-loop of AURKA and thereby activates AURKA lacking phosphorylation on its T-loop [50] (**Fig. 1A,** left panel). In turn, AURKA phosphorylates the T-loop of Plk1, thereby activating its catalytic function. The structural basis for this unique mechanism of kinase regulation remains to be determined**.**

Here, we sought to dissect how phospho-Bora binds and activates unphosphorylated AURKA and how this activated form of AURKA can target Plk1. By combining AlphaFold structural modelling and extensive structure-function analysis, we provide evidence that phospho-Bora wraps around the N-terminal lobe of AURKA to position its essential phospho-Serine 112 towards the activation loop of AURKA. More importantly, we show that the T-loop of Plk1 is impervious to AURKA phosphorylation in the absence of pBora. However, by interacting with the Alpha C helix of the Plk1 kinase domain through an evolutionarily conserved motif, pBora focuses AURKA activity towards the Plk1 T-loop. We demonstrate the importance of this conserved motif in Bora for mitotic entry in

Xenopus egg extracts. Phospho-Bora thus selectively activates and localizes AURKA close to Plk1 to trigger its activation and mitotic entry. Our results describe the molecular basis of mitotic kinase activation, which provides insights into how cells meet the challenge of spatially and temporally limiting Plk1 activation during mitosis.

Results:

Inserting the phosphorylated [PpSP] M3 motif of Bora within Tpx2 is sufficient to potentiate non-phosphorylated AURKA kinase activity

Sequence comparison with Tpx2 revealed two putative short AURKA-binding motifs in Bora, the M1 [amino acids 22-35] and M2 [100-109] motifs (**Fig. 1B,** left panel) [50]. Notably, the Bora M2 motif is relatively well conserved between Bora (**Fig. 1B**, left panel) and Tpx2 (**Fig. 1B**, right panel) and is located immediately N-terminal to the essential pSer112 (M3 motif) (**Fig. 1B**). Assuming that the M2 motif of Bora engages AURKA similarly to the M2 motif of Tpx2 (**Fig. 1A,** right panel) [44], we hypothesized that the phosphate of the M3 motif of Bora would be positioned towards the active site of AURKA, allowing it to functionally replace the missing phosphate on the T-loop "*in trans*", which is typically supplied by autophosphorylation [42]. This would stabilize the kinase near the active site, thereby potentiating kinase activity [50,59].

To test this hypothesis, we fused the M3 phospho-motif of Bora to the first 41 amino acids of Tpx2 to generate a phosphorylated pTpx2-Bora chimera (**Fig. 1B,** phosphopeptide MK51). We then tested whether the phosphate of the M3 motif increased Tpx2 affinity for unphosphorylated AURKA (i.e., AURKA^{T288V}, mimicking unphosphorylated AURKA). Using a competitive displacement binding assay with fluorescein-labeled Tpx2 (**Fig. 1C**) [59], we observed that the pTpx2-Bora chimera displaced the interaction between FITC-Tpx2 and AURKA^{T288V} more efficiently (~3 fold) than Tpx2, as measured by fluorescence polarization. This indicated that the pTpx2-Bora chimera bound more tightly than Tpx2 to AURKA^{T288V} (**Fig. 1C**). By contrast, a phosphopeptide directly fusing the putative M1, M2, and M3 motifs of Bora (**Fig. 1B,** phosphopeptide GK51) failed to displace the interaction between FITC-Tpx2 and AURKA^{T288V} (**Fig. 1C**). This observation suggests that while Tpx2 and Bora share some sequence similarities and can compete for AURKA binding [59], their binding mode to AURKA likely differs to some extent.

Next, we tested the potentiating effect of the pTpx2-Bora chimera on AURKA^{T288V} kinase activity towards the model Kemptide substrate by monitoring the consumption of ATP with the ADP-glo assay [62]. This assay quantifies the amount of ADP produced during a kinase reaction (**Fig. 1D**). AURKA^{T288V} in the presence of non-phosphorylated Bora displayed negligible activity, consistent with our previous observations [59]. However, the addition of the phosphorylated Tpx2-Bora chimera potentiated the activity of AURKA^{T288V} multifold (**Fig. 1D**). In fact, the EC_{50} value for potentiation by pTpx2-Bora was similar to phosphorylated Bora (45 +/- nM vs. 71 +/- nM, respectively). In contrast,

the phosphopeptide, obtained by directly fusing the putative M1, M2, and M3 motifs of Bora, failed to activate AURKA^{T288V,} consistent with the binding experiments (**Fig. 1D**). These observations support our hypothesis that the M2 motif of Bora positions the essential phospho-motif M3 in the active site of AURKA, enabling the phosphate on Bora S112 to functionally replace the phosphate on T288.

The pTpx2-Bora chimera potentiates AURKA^{T288V} kinase activity but lacks the determinants needed to direct AURKA^{T288V} activity toward the Plk1 kinase domain

As the pTpx2-Bora chimera potentiates AURKA^{T288V} activity toward the artificial kemptide substrate, we next tested whether it also activates AURKA^{T288V} toward Ser 10 of Histone H3 [63] and the Plk1 kinase domain (kinase-dead (K82R) but phosphorylable on the T210 (hereafter Plk1^{Kdom})) [10,41,59]. The pTpx2-Bora chimera, similarly to pBora, readily potentiated AURKA^{T288V} activity toward Histone H3, in line with the results obtained with the Kemptide substrate (**Fig. 2A**). However, in marked contrast to pBora, the chimeric pTpx2-Bora construct failed to stimulate AURKA^{T288V} activity toward the Plk1 kinase domain (**Fig. 2B,** compare pT210 phosphorylation between lanes 1-6 and 7-12). Hypothesizing that the Plk1 T-loop might not be accessible within the kinase domain, we asked whether the pTpx2-Bora chimera could activate AURKA^{T288V} towards the isolated Plk1 T-loop (aa 190-225) fused to GST (hereafter GST$^{T\text{-}loop}$). At first glance, the pTpx2-Bora chimera appeared to activate AURKA^{T288V} toward the isolated Plk1 T-loop similarly to pBora (**Fig. 2C).** However, to further compare the efficiency of pBora and the pTpx2-Bora chimera at promoting Plk1 T-loop phosphorylation by AURKA^{T288V}, whether the T-loop is embedded in the Plk1 kinase domain or isolated, fused to GST, we ran the 30 and 60-minute time-points of the kinase assays side-by-side on the same SDS-PAGE. As shown in **Fig. 2D**, pBora and the pTpx2-Bora chimera activated AURKA^{T288V} toward the GST$^{T\text{-}loop}$ but with poor efficacy compared to the effect observed with pBora on AURKA^{T288V} when the Plk1 kinase domain was used as a substrate (**Fig. 2D,** compare lanes 2, 3 with lanes 8, 9 and 11, 12).

Taken together, these results suggest that pBora contains unique determinants, which are absent in the shorter pTpx2-Bora chimera, that allow unphosphorylated AURKA to phosphorylate the Plk1 T-loop, which is intrinsically a poor substrate for AURKA (**Fig. 2E**). These findings align with our previous observation that AURKA cannot phosphorylate Plk1 in the absence of pBora [59].

AlphaFold 3 structural modeling predicts that Bora$^{18-120}$ wraps around the N-terminal lobe of AURKA to position the phospho-Ser112 motif in the active site of AURKA

Next, we investigated how pBora activates unphosphorylated AURKA towards the Plk1 kinase domain. Compared to Tpx2, the minimal Bora fragment that activates unphosphorylated AURKA is considerably larger, spanning residues 18 to 120, with a conserved region between the M1 and M2 motifs unique to Bora, hereafter named the Bora-Specific Motif (BSM) (**Fig. 3A**) [59]. Understanding the binding mode of pBora to AURKA requires the structural characterization of the pBora$^{18-120}$•AURKA complex. However, despite several attempts, we did not obtain a crystal structure of the minimal phosphorylated Bora$^{18-120}$ fragment bound to AURKA^{T288V}, possibly due to the intrinsically disordered nature of Bora [59]. Therefore, we utilized the AlphaFold3 (AF3) algorithm to predict the interaction mode between phospho-Bora$^{18-120}$ and AURKA, comparing it to other allosteric activators in complex with AURKA, including Tpx2 (PDB: 1OL5 [http://DOI:10.2210/pdb1OL5/pdb]) [44,64], Cep192 (PDB: 8PR7 [https://doi.org/10.2210/pdb8PR7/pdb]) [65], (PBD: 8GUW [https://doi.org/10.2210/pdb8GUW/pdb] [66] and TACC3 [PDB: 5ODT https://doi.org/10.2210/pdb5ODT/pdb]) [67], for which 3D structures are available.

The crystal structure of the AURKA•Tpx2$^{1-43}$ complex showed that Tpx2$^{1-43}$ binds AURKA using two separate motifs, the M1 (residues 7-21) and the M2 motifs (residues 30-43), which are connected by a flexible linker. The M1 motif is extended and uses hydrophobic plugs (Y8, Y10, F16, F19) to bind two hydrophobic pockets on the N-lobe of AURKA called the Y and F pockets, respectively (**Fig. 3B**) [44,64]. Of note, Cep192, which promotes AURKA autophosphorylation at centrosomes [68], also engages the F-pocket of AURKA via two aromatic anchors (Y487 and F490, equivalent to F16 and F19 in Tpx2) [65].

In contrast to the extended M1 motif, the Tpx2 M2 motif (residues 30 to 43) adopts an alpha-helical conformation that binds between the N- and C-terminal lobes of AURKA, adjacent to the helix αC and to the activation segment via aromatic residues, W34 and F35, which engage the W pocket of AURKA [44,64] (**Fig. 3B**). Tpx2 preferentially binds phosphorylated AURKA and induces conformational changes within the catalytic infrastructure and the T-loop, such that the phosphorylated T288 residue contacts several arginine residues, thereby stabilizing the activation loop (**Fig. 3C**) [44,45,64].

In five out of five generated models, AF3 predicts a different mode of interaction between Bora$^{18-120}$ and AURKA (**Fig. 3D** and **S1A**). In contrast to Tpx2$^{1-43}$, which binds

along the same face of the kinase N-terminal lobe (**Fig. 3B**), Bora$^{18-120}$ wraps circuitously around the N-terminal lobe of AURKA (**Fig. 3D** and **S1A**). The putative M1 motif of Bora binds the same face of AURKA as observed for the M1 motif of Tpx2. However, the M1 region in Bora is much larger than initially anticipated (extending from residues L22 to F45 rather than 22 to 35) based on structural alignments [59] and is oriented in the opposite direction compared to that observed for Tpx2$^{1-43}$ (**Fig. 3B, 3D**). Despite this difference, two hydrophobic anchors in Bora (F25 and V44-F45) are predicted to bind the same hydrophobic F and Y pockets of AURKA as observed for Tpx2$^{1-43}$ (**Fig. 3D**). Following the Bora M1 motif, the evolutionarily conserved Bora-specific motif located between T52 and I78 (**Fig. 3D**) binds at the back of AURKA N-terminal lobe (**Fig. 3F**). In particular, the conserved I60 and I71 residues are predicted to dock on two pockets at the back of AURKA N-terminal domain (**Fig. 3F**). Noteworthy, the other allosteric AURKA activators TACC3 and Cep192 also bind these two pockets of AURKA [65-67] (**Fig. S1B, S1C**). While I60 and I71 residues anchor Bora to AURKA, other highly conserved aromatic or hydrophobic residues, such as F56, W58, and I66, are conspicuously solvent-exposed in this conserved region (**Fig. 3F**, red arrows).

After Bora$^{18-120}$ circles the N-terminal lobe of the kinase, the α-helical M2 motif is similarly positioned to that observed in Tpx2$^{1-43}$. This segment contains conserved aromatic residues F103 and F104, equivalent to W34 and F35 in Tpx2, and they dock in the hydrophobic W pocket of AURKA while packing against the alpha C helix (**Fig. 3D**). Next, the Bora M2 motif positions the pS112 M3 motif in the AURKA active site, allowing it to substitute in *trans* for the phosphate typically provided by autophosphorylation. The phospho-site is predicted to interact with the “arginine pocket” of AURKA, composed of R255, R180, and R286 (**Fig. 3E**), which has been previously shown to bind the phosphate on the T288 residue of the T-loop, particularly when phospho-AURKA is bound to Tpx2$^{1-43}$ (**Fig. 3C**) [44]. The model also predicts that AURKA bound to pBora exhibits characteristics of an active kinase with the “DFG motif in” and the R-spine assembled (**Fig. S1D**).

Overall, this binding model is consistent with previous observations that Bora and Tpx2 compete for AURKA binding [59,69], that the “Arginine pocket” is required for high-affinity binding of pBora to AURKA^{T288V} [59], and our present results showing that providing a phosphosite to Tpx2 is sufficient to increase its affinity for unphosphorylated AURKA and to potentiate AURKA kinase activity (**Fig. 1C, 1D**).

A streamlined method for high-throughput screening of the critical determinants of phospho-Bora and AURKA-dependent Plk1 T-loop phosphorylation in *E. coli*

To test our AlphaFold model, we generated Bora variants mutated on evolutionarily conserved residues and residues predicted to contact AURKA (**Fig. 3**).

To assess Bora's function, we previously used a two-step kinase assay with purified proteins in which, in the first step, we treated Bora with active Cyclin A-Cdk1 or the Mitogen-Activated Protein (MAP)-kinase ERK, to phosphorylate the essential M3 motif pS112 in Bora. In a second step, we then added AURKA^{T288V} and a kinase-dead mutant of the Plk1 kinase domain (K82R), which can still be phosphorylated on its T-loop as substrate. Western blotting of the reaction allowed the monitoring of Plk1 T210 phosphorylation as a direct readout of AURKA^{T288V} activity stimulated by pBora [50,57,58]. However, testing multiple Bora variants by this approach would require systematic purification and pre-phosphorylation for each. To circumvent this bottleneck and to rapidly screen the activity of the phosphorylated Bora variants, we developed a streamlined method that we named MITOKINAC, for MITOtic KINases Activation in *E. Coli* (**Fig. 4A**). This method reconstitutes pBora-dependent activation of non-phosphorylated AURKA (AURKA^{T288V}) and then Plk1 T-loop phosphorylation directly in *E. coli,* without the need to purify the proteins, as summarized in **Fig. 4B**. Briefly, we co-transformed *E. coli* BL21 with three plasmids expressing i) the active ERK kinase (or ERK kinase dead as control), which replaces Cyclin A-Cdk1 as a Proline-directed kinase to phosphorylate the M3 motif of Bora, ii) Bora$^{1-224}$ WT or S112A as control, and AURKA^{T288V} expressed from the same plasmid, and iii) the Plk1 kinase domain as a substrate (kinase-dead K82R but phosphorylable on the T-loop (T210)) (**Fig. 4A**). After protein induction, Plk1 T-loop phosphorylation was monitored by Western-blot directly on total bacterial extracts using a specific antibody directed against the phospho-Threonine 210 of Plk1 (anti-pT210).

In this assay, wild-type pBora stimulated AURKA^{T288V} activity towards the Plk1 T-loop (**Fig. 4C** lane 3). Importantly, Plk1 T-loop phosphorylation was strictly dependent on the presence of Bora phosphorylated on the M3 motif pS112 by active ERK (**Fig. 4C,** compare lane 3 with lanes 1, 2, and 4). Indeed, no Plk1 T-loop phosphorylation was detected in the absence of Bora (**Fig. 4C**, Lane 1), or when ERK was replaced with a kinase dead variant (Lane 2), or when Bora was mutated on the critical S112 residue (Lane 4).

The system's versatility enables rapid screening for Bora, AURKA, and Plk1 variants. For instance, we substituted the Plk1 kinase domain with the isolated Plk1 T-loop fused

to GST as an alternative AURKA substrate and observed that pBora enhances AURKA^{T288V} activation towards this target, albeit with relatively poor efficacy since the GST-T-loop is significantly overexpressed in *E. coli*, compared to the Plk1 kinase domain (**Fig. 4D**). Again, this reaction was strictly dependent on the presence of Bora phosphorylated on the M3 motif pS112 by active ERK (**Fig. 4D**, compare lane 3 with lanes 2 and 4).

To corroborate these observations and further exploit MITOKINAC, we used Genetic Code Expansion [70-72] to insert a PhosphoSerine directly at position 112 of Bora during translation in *E. coli,* thereby bypassing the need for priming phosphorylation by ERK [59] (**Fig. 4E**). As shown in **Fig. 4F**, directly inserting a phosphoSerine specifically at position 112 of Bora$^{1-224}$ during translation promotes AURKA^{T288V} activation towards the Plk1 T-loop (**Fig. 4F**). In line with previous results, no activation was observed using Bora$^{1-224}$ non-phosphorylated, demonstrating that phosphorylation of this S112 position is necessary and sufficient for Bora's function.

Overall, this method is ideally suited for rapidly screening critical determinants required for the activation of unphosphorylated AURKA by phospho-Bora towards the Plk1 kinase domain. More generally, this method can be implemented to study any kinase activation cascade or kinase-substrate relationship [73].

The extended Bora M1 motif binds the hydrophobic Y and F pockets of the N-terminal lobe of AURKA via two aromatic plugs

We next used MITOKINAC to screen 39 mutant variants (affecting 35 unique amino acids) within the Bora$^{18-120}$ fragment for their ability to promote AURKA^{T288V} phosphorylation of the Plk1 kinase domain. Although we expressed the first 224 amino acids of Bora in *E. coli*, we mutagenized only the region between amino acids 18 and 120 because it is the only part of Bora predicted by AF3 to bind AURKA. We systematically substituted hydrophobic residues with acidic residues and charged residues with residues of opposite charge.

Based primarily on sequence alignment between Tpx2 and Bora, we had previously predicted that residues F25 and Y31 in Bora might fulfill a similar function to the aromatic plugs of Tpx2 in binding AURKA. Indeed, the double Bora F25D Y31D mutant was inactive and failed to displace the Tpx2-AURKA interaction [59]. Here, we screened several additional positions within the extended M1 motif of Bora (amino acids 22-48) (**Fig. 5A, B, C**) and found that F25D (**Fig. 5B**, lane 5) but not Y31D (lane 9) and the double V44D, F45D (lane 20) mutations affected Bora's ability to activate AURKA^{T288V}

towards the Plk1 T-loop. Substitution of F25 by Aspartic acid eliminated Bora's function, whereas the single V44D and F45D substitutions had no detectable effect (**Fig. 5B,** compare lanes 5, 11, 12, and 20). We only observed reduced Plk1 T-loop phosphorylation by AURKA^{T288V} when both V44 and F45 were substituted by Aspartic acid. We confirmed these results using purified proteins and *in vitro* kinase assays (**Fig. 5D,** compare lanes 2, 4, 6, and 8).

These observations are entirely consistent with the AlphaFold 3 model, which predicts that Bora's extended M1 motif binds AURKA via the two hydrophobic plugs, F25 and V44-F45, which engage the hydrophobic F and Y pockets of AURKA, respectively, in an opposite orientation compared to Tpx2 (**Fig. 3B, D**) with F25 playing a more significant role. These results also align with recent data showing that a 20 amino-acid Bora fragment (aa 18-38) encompassing F25, which is part of an "NPF" motif (aa 23-25), is sufficient for AURKA binding [74].

The M2 motif positions the essential phospho-motif in the active site of AURKA via hydrophobic anchors

Next, we focused on the M2 motif, located upstream of the essential phospho-Serine S112, or M3 motif. Based on AF3, the α-helical M2 motif is similarly positioned to the M2 motif of Tpx2$^{1-43}$. This segment contains the conserved aromatic residues F103 and F104, which are equivalent to W34 and F35 in Tpx2, docking on the hydrophobic W pocket of AURKA (**Fig. 3**). We previously reported that the double Bora F103D F104D mutant phosphorylated on the M3 motif does not bind and activate AURKA^{T288V} [59]. Here, using MITOKINAC and then *in vitro* kinase assays, we found that individually mutating F103 and F104 residues is sufficient to abrogate Bora's function, highlighting the critical role of these two residues (**Fig. 5E, F G, H**). Mutation of the I109 and V110 residues also affected Bora's function (**Fig. 5E, F**), most likely by preventing the proper positioning of the phosphoSerine 112 in the active site of AURKA or, in the case of V110R, by inhibiting S112 phosphorylation by ERK. Accordingly, the Bora V110R variant was not upshifted on SDS-PAGE (as Bora S112A (**Fig. 5F**), suggesting that ERK did not efficiently phosphorylate this variant.

These results identify the key Bora residues in the M1 and M2 motifs that are critically required for AURKA activation.

The Bora-specific motif (aa 52-78) dictates AURKA's specificity towards the Plk1 kinase domain

We next screened the highly conserved region (amino acids 50-78) between the M1 and M2-M3 motifs, which is specific to Bora (**Fig. 6A**). Using MITOKINAC, we found that mutation of several conserved residues, including F56, W58, S59, I60, I66, P68, V69, I71, I76, and Q79 affected Bora's ability to promote AURKA^{T288V} phosphorylation of the Plk1 T-loop embedded in the kinase domain (**Fig. 6A**, **6B**). Intriguingly, several of these mutations had no effect when only the isolated Plk1 T-loop fused to GST was used as a substrate (**Fig. S2B**). Indeed, in contrast to Bora F25D, which is defective for promoting AURKA^{T288V} phosphorylation of both the Plk1 kinase domain and isolated Plk1 T-loop substrates, the Bora variants, F56D, W58D, S59R, I60D, Q62R, and I66D, retained the ability to promote AURKA^{T288V} phosphorylation of the isolated Plk1 T-loop in *E. coli* (**Fig. S2B**).

Based on AF3 structural modeling, this region is predicted to bind AURKA at the back of the molecule (**Fig. 3D**). The Serine 59, which is part of an AURKA consensus site (RWS) [75] and previously shown to be phosphorylated by AURKA itself [76], is the first residue of a predicted alpha-helix, also known as the N-cap residue. Substitution of this Serine by an Arginine abrogated Bora's ability to promote AURKA^{T288V} phosphorylation of the Plk1 kinase domain. However, substituting this Serine with a Glutamic acid as the helix's N-cap residue had no discernible effect (**Fig. 6B**).

Next to Serine 59, Isoleucine 60 at the beginning of the Bora-specific motif (**Fig. 6A**) and Isoleucine 71 at the end anchor the motif into two pockets of AURKA that TACC3 and CEP192 also use to bind AURKA (**Fig S1B, S1C**) [65-67]. However, other conserved residues essential for Bora's function, including F56, W58, and I66, are solvent-exposed and are not predicted to bind AURKA (**Fig. S2A**). We reasoned that some of these residues, absent from the smaller pTpx2-Bora chimera (**Fig. 1B**), might confer AURKA specificity to the Plk1 kinase domain.

To test this hypothesis, we purified these Bora variants and then compared their ability to activate AURKA^{T288V} toward the Plk1 kinase domain, the isolated Plk1 T-loop, and Histone H3 using *in vitro* kinase assays. Consistent with the results obtained using MITOKINAC, all these Bora variants failed to promote AURKA^{T288V} phosphorylation of the Plk1 kinase domain (**Fig. 6C, 6D**), but retained their ability to promote AURKA^{T288V} phosphorylation of the isolated Plk1 T-loop (**Fig. 6E, 6F**) or Histone H3 (**Fig. 6G, 6H**).

At face value, these observations suggest that this evolutionarily conserved region of Bora is not essential for AURKA^{T288V} kinase activation per se but is required to direct AURKA specificity towards the Plk1 kinase domain.

Bora docking to the Plk1 kinase domain promotes T-loop phosphorylation by AURKA

Our observations thus suggest that pBora not only activates non-phosphorylated AURKA by bypassing the need for T-loop autophosphorylation, but it also allows AURKA to selectively phosphorylate the T-loop of Plk1 in the context of an intact kinase domain, possibly via the conserved and possibly solvent-exposed residues of the Bora-specific motif. To investigate this possibility further, we interrogated AlphaFold3 for potential interactions between Bora and the Plk1 kinase domain by modeling the AURKA•Plk1 kinase domain•Bora$^{18-120}$ trimeric complex.

Although Bora phosphorylated on its Polo-docking site (S252) by Cyclin-Cdk robustly binds the Plk1 PBD (Polo-box domain) [69,77], we never detected a stable interaction between Bora and the Plk1 kinase domain by pull-down experiments or NMR studies [59]. However, AF3 predicts an interaction between the Bora-specific motif and the helix alpha C of the Plk1 kinase domain (**Fig. 7A**). The total interaction area is 554 Å^2. It involves contact between several residues of the Bora-specific motif, including W56, F58, I66 **(Fig. 7B),** and R48, R95, R106A, E121A of the Plk1 kinase domain (**Fig. 7C**). To assess the significance of the predicted interaction between pBora and the Plk1 kinase domain, we purified mutants of the Plk1 kinase domain and tested them as substrates of pBora•AURKA^{T288V} using in vitro kinase assays. Notably, mutations in the Plk1 residues R48, R95, R106, and E121 reduced the pBora and AURKA-dependent phosphorylation of the Plk1 T-loop.

Together, these results strongly suggest that transient interaction between Bora and the Plk1 kinase domain is required for the ability of AURKA to efficiently phosphorylate the Plk1 T-loop.

The Bora-specific motif is critically required for mitotic entry in Xenopus egg extracts

Having determined that the Bora-specific motif is essential for Bora's function *in vitro*, we next investigated the relevance of this determinant in a physiological context. To this end, we tested Bora's function during mitotic entry in Xenopus egg extracts, whereby interphase egg extracts are forced to enter into mitosis using the hyperactive Gwl^{K72M}

kinase [60,78]. Indeed, adding a recombinant hyperactive human Gwl kinase (Gwl^{K72M}) to interphase extracts partially inhibits the phosphatase PP2A-B55, stabilizing substrate phosphorylation by basal Cyclin-Cdk activity, which forces entry into mitosis [78]. However, prior immunodepletion of Bora from these extracts prevents mitotic entry [59,60]. Under these conditions, Plx1 (Xenopus Plk1) activation by AURKA and the dephosphorylation of the inhibitory phosphorylation on Cdk (specifically on Tyr15) are inhibited. This mitotic entry defect can be fully rescued by adding wild-type recombinant Bora [59,60] (**Fig. 8A**). We therefore tested whether the minimal Bora fragment 18-120 that supports Plk1 phosphorylation by AURKA *in vitro* could promote mitotic entry in interphase extracts depleted of Bora. We again use the MAPK kinase ERK to pre-phosphorylate Bora on S/T-P sites, as we did in our *in vitro* reactions, to circumvent inefficient phosphorylation of Bora fragments by Cyclin A-Cdk1 in Xenopus egg extracts. As shown in **Fig. 8B**, the wild-type $Bora^{18-120}$ fragment, pre-phosphorylated by ERK rescued mitotic entry as revealed by the accumulation of mitotic markers, including the phosphorylation of the Gwl kinase, the phosphorylation of Plx1 on the T-loop (T201), and the dephosphophorylation of the inhibitory site on the Tyrosine 15 of Cdk1. By contrast, none of the Bora variants tested rescued immunodepletion of Bora. Taken together, these results indicate that the Bora determinants required for Plk1 binding are essential for mitotic entry in Xenopus egg extracts.

Discussion

By integrating AlphaFold structure modeling with extensive structure-function analysis, we discovered that the intrinsically disordered protein Bora acts as a unique and selective activator of Plk1 T-loop phosphorylation by AURKA. We show that once phosphorylated, Bora not only activates unphosphorylated AURKA by delivering a critical phosphosite near the T-loop *in trans* to functionally replace the phosphate normally provided by T-loop autophosphorylation, but it also selectively directs AURKA's kinase activity towards the Plk1 T-loop by interacting with the alpha C helix of the Plk1 kinase domain. pBora thus directs AURKA activity specifically to the Plk1 kinase domain, which is otherwise a poor substrate for AURKA. We have identified the specificity determinants in a conserved region of Bora that tethers AURKA to the Plk1 kinase domain, positioning AURKA's active site close to its substrate. Furthermore, we confirmed the importance of these determinants for Bora's function during mitotic entry in Xenopus egg extracts. Our findings reveal important details about the molecular mechanisms that drive mitotic kinase activation during mitosis, potentially explaining how cells manage the challenge of limiting Plk1 kinase activity in space and time.

AF3 predicts that the minimal Bora$^{18-120}$ fragment wraps around the N-terminal lobe of AURKA to position the activating phosphate in the T-loop of AURKA

While it is well established that Bora physically binds to and activates AURKA [56,59,79], the mode of interaction remains unclear. Based on protein sequence alignments, we previously reported that Bora$^{18-120}$ shares some AURKA-binding elements with Tpx2$^{1-43}$, particularly aromatic residues in the M1 and M2 motifs. Accordingly, Bora$^{18-120}$ and Tpx2$^{1-43}$ compete for AURKA binding, and these aromatic residues are crucial for this competition [59]. The AlphaFold 3 model of the pBora$^{18-120}$ -AURKA complex, thoroughly tested through our structure-function analysis, confirms and extends these observations by providing key additional insights. First, the model predicts that the M1 motif of Bora$^{18-120}$ (aa 22-45) is longer than expected and binds to the AURKA N-terminal lobe in an opposite orientation compared to Tpx2$^{1-43}$, with F25 binding to the F-pocket and V44 and F45 binding to the Y pocket of AURKA. This explains why the Bora M1-M2-M3 fusion failed to activate AURKA^{T288V} in ADP Glo assay (**Fig. 1C, 1D**), as it contains only an incomplete version of the M1 motif (aa 22-40), directly linked to the M2 motif, and thus the binding elements cannot engage AURKA correctly. Second, AF3 predicts that Bora$^{18-120}$ wraps around the N-terminal lobe of the kinase domain. On the other side of AURKA from the M1 and M2 binding motifs, pBora$^{18-120}$ binds to two AURKA pockets

through the hydrophobic residues I60 and I71, which are also critical for Bora's function. Notably, previous structural studies have shown that these same two pockets are utilized by Cep192 [65,66] and TACC3 [67] to bind AURKA, suggesting that all these allosteric activators will compete for AURKA binding. This would help ensure their sequential (and not concomitant) action during mitotic entry and progression. After Bora$^{18-120}$ wraps around the N-terminal lobe of AURKA, the M2 motif is similarly positioned to that observed for Tpx2, and we demonstrated that F103 and F104 residues in this motif are critically required for Bora's function. These residues anchor the M2 motif to the W pocket of AURKA and position the phospho-M3 motif in the active site of AURKA. AF3 predicts that the phospho-motif M3 binds to the pocket composed of three arginine residues (R180, R255, and R286), a site normally occupied by the phosphorylated (pT288) T-loop [44]. Thus, the M3 motif influences AURKA catalytic function (as observed for the phosphorylation of the T-loop) by stabilizing a productive conformation of the activation segment, a function normally supported by AURKA T-loop phosphorylation. Our finding that fusing the phospho-M3 motif of Bora to Tpx2 is sufficient to potentiate AURKA^{T288V} catalytic activity further supports this hypothesis.

The Bora-AURKA complex is a unique Plk1 activator during mitotic entry and progression

AURKA is characterized as an "incomplete" kinase because it relies heavily on its sequential interaction with various regulators to achieve maximal activity during mitotic entry and progression. These regulators localize to different places where they recruit and activate different forms of AURKA [9,49,59]. In the cytoplasm, before nuclear envelope breakdown, Bora, phosphorylated by Cyclin A – Cdk1, preferentially binds to and activates unphosphorylated AURKA, which is kept dephosphorylated by the PP1 and PP2A phosphatases. Here, we show that beyond activating AURKA, Bora specifically recruits its substrate Plk1. By binding both AURKA and Plk1, pBora focuses AURKA's activity on its substrate and likely facilitates the optimal positioning of the phosphoacceptor residue of Plk1, close to the active site of AURKA. Without Bora, AURKA cannot phosphorylate the Plk1 T-loop [59]. The interaction between Bora and the Plk1 kinase domain is essential for the efficient phosphorylation of the Plk1 T-loop by AURKA. Consistently, the pTpx2-Bora chimera, which lacks the binding elements to the Plk1 kinase domain, activated unphosphorylated AURKA toward kemptide and Histone H3 robustly but failed to activate AURKA toward the Plk1 kinase domain. Similarly, pBora was inefficient at activating AURKA toward the isolated Plk1 T-loop, highlighting

the importance of the transient interaction between this evolutionarily conserved region of Bora and Plk1. Our results show that the Plk1 T-loop is a poor substrate for AURKA. However, by concentrating active AURKA on the Plk1 kinase domain, pBora facilitates the phosphorylation of this impervious T210 site by AURKA.

Extending these observations, Esposito Verza et al., in the accompanying manuscript, unequivocally demonstrate that the sequence surrounding the phosphorylated T210 residue of the Plk1 T-loop is a sub-optimal consensus phosphorylation site for AURKA-mediated phosphorylation ([R-K-K-pT] instead of [R-R-X-pT/S]). Accordingly, a single K to R substitution in the -2 position is sufficient to convert the Plk1 T-loop into an optimal AURKA substrate. These observations, together with our data, indicate that the AURKA•Bora complex is unique in phosphorylating the Plk1 T-loop during mitotic entry and progression.

Limiting Plk1 activation during mitosis

What are the functional implications of these observations? Plk1 is crucial for mitotic entry and progression. Plk1 regulates mitotic entry, centrosome assembly and maturation, nuclear envelope breakdown, chromosome condensation, kinetochore function, and cytokinesis. Its activity must, therefore, be tightly controlled in space and time. Our results indicate that Plk1 T-loop phosphorylation by AURKA is inefficient and largely relies on phospho-Bora. This mechanism, together with the extensive Plk1- and ubiquitin-mediated degradation of phospho-Bora [69,77], may prevent uncontrolled Plk1 activation in the absence of signaling from Cyclin A/B–Cdk1. Both mechanisms may work in concert to maintain low levels of phosphorylated and, thus, active Plk1 during mitosis. Deregulation of these mechanisms, such as an accumulation of phosphorylated Bora, may lead to hyperactivation of the AURKA-Plk1 axis with detrimental consequences. Accordingly, Bora overexpression has been linked to oncogenic transformation and cancers with poor prognosis [80-82]. This work may, thus, pave the way for developing inhibitors of this pathway with therapeutic potential.

Limitations of the study

Although we extensively tested the structural models predicted by Alphafold 3, the position of the residues we have mutated has not yet been observed experimentally using high-resolution structural biology methods. In addition, as mentioned above, outside the minimal active Bora$^{18-120}$ fragment, other regions potentially contributing to the assembly of the trimeric AURKA•pBora•Plk1 complex *in vivo* were not modeled

here. In particular, the interaction between the Plk1 PBD domain and Bora phosphorylated at the Polo-docking site (S252). Finally, the stoichiometry of the interaction between the partners is undetermined. We modeled it 1:1:1, but a more complex assembly might form *in vivo*.

Acknowledgments

We thank P. Moussounda for helping with media preparation. R. Karess for the critical reading of the manuscript. We are grateful to Marc Plays and the ZEFIX animal facility for antibody production. We thank A. Esposito-Versa and A. Musacchio for discussions and for sharing results before publication. AP is supported by a PhD Fellowship from La “Ligue Nationale Contre le Cancer”. CBC is supported by a PhD Fellowship from CBS2 Montpellier University. NJ is supported by a grant from the Fondation ARC pour la Recherche sur le Cancer (ARCPJA2022050005002) and a grant from Université Paris-Cité IDEx (ANR-18-IDEX-0001, “Emergence en Recherche” RS30J23IDX64_KATAREP). Work in the laboratory of TL is supported by grants from “Agence Nationale pour la Recherche” (ANR, France – MITODISSECT, ANR-22-CE13-0022) and by the « fondation ARC », ARC 2023 PJA3. Work in the laboratory of FS is supported by a Canadian Institutes of Health Research grant (PJT-178026) and a Terry Fox Research Institute grant (TFRI-1107-04). Work in the laboratory of LP is supported by grants from “Agence Nationale pour la Recherche” (ANR, France – MITODISSECT, ANR-22-CE13-0022), by the IdEx Université Paris Cité, ANR-18-IDEX-0001 and by the “Ligue Nationale Contre le Cancer” (Equipe labéllisée, France).

The authors declare that they have no conflict of interest.

Material and Methods:

Molecular biology and DNA manipulation

All the DNA constructs were generated by Gateway (Invitrogen) or with restriction enzymes. All DNA constructs were verified by DNA sequencing. Oligonucleotides used for site-directed mutagenesis were purchased from Eurofins Genomics and are detailed in the **Supplementary Table 2**. The list of plasmids used in this study is provided in **Supplementary Table 1**.

pET-His6-ERK2-MEK1_R4F_coexpression was a gift from Melanie Cobb (Addgene plasmid #39212; http://n2t.net/addgene:39212; RRID: Addgene_39212). The plasmid pKW2 : SepRS(2)/pSertRNA(B4)/EF-Sep was a gift from Jason W Chin (Addgene plasmid #173897; http://n2t.net/addgene:173897; RRID: Addgene_173897), Machinery plasmid for pSer incorporation, chloramphenicol resistance/pBR322 origin of replication (Rogerson et al., 2015).

MITOKINAC

Escherichia coli BL21 DE3 RIL (Thermo Fischer Scientific) chemically competent bacteria were co-transformed with three plasmids expressing i) active ERK (pET-His6-ERK2-MEK1_R4F), ii) StrepTag-AURKA^{T288V} in operon with Bora$^{1-224}$-6xHis WT or mutants, and iii) GST-Plk1$^{1-330\ K82R}$ (kinase-dead).

Transformants were selected on LB plates containing Kanamycin (30 µg/ml), Ampicillin (50 µg/ml), and Streptomycin (30 µg/ml) after overnight incubation at 37°C. Colonies were then inoculated in LB medium containing Kanamycin (30 µg/ml), Ampicillin (50 µg/ml), and Streptomycin (30 µg/ml) until the culture reached OD_{600}=1-1.5. All the cultures were then diluted in fresh media at OD_{600}=0.1, and grown until they reached OD_{600}=0.6-0.8. Next, protein expression was induced using 0.5 mM IPTG for 3 hours at 25°C. After protein induction, the optical density (OD) of the culture was measured, and 500 µL of bacteria were collected by centrifugation for 5 minutes at 11,000 g and resuspended directly in Laemmli Buffer to reach a concentration of 5 mOD/µL. 10 µl (50 miliOD) were then analyzed by SDS-PAGE and Western blot.

MITOKINAC using Genetic Code Expansion to produce pSer112 Bora$^{1-224}$

For the production of Bora$^{1-224}$-6xHis incorporating phosphoserine at Ser112, BL21 B95 (DE3) ΔA ΔfabR ΔserB bacteria were used (Addgene #197655).

In the first step, chemically competent bacteria harboring the plasmid pKW2-EF-Sep (Addgene #173897), which contains an orthogonal aminoacyl-tRNA synthetase/tRNACUA pair, which directs the efficient incorporation of phosphoserine (pSer) into recombinant proteins, were generated.

These bacteria were then co-transformed with pLP2855 and pLP2228 by heat shock for 45 seconds at 42°C, followed by recovery in 1 ml SOC medium for two hours at 37°C. Co-transformants were selected on an LB plate containing 12.5 µg/ml kanamycin, 12.5 µg/ml streptomycin, and 7 µg/ml chloramphenicol for 24 hours at 37°C. They were then inoculated for an overnight culture in LB with 25 µg/ml kanamycin, 25 µg/ml streptomycin, and 14 µg/ml chloramphenicol. The culture was diluted to OD_{600}=0.1, and protein expression was induced by IPTG for 3 hours at 25°C and processed as described above.

Recombinant protein expression

Full-length AURKA^{T288V}, Plk1$^{1-330}$ kinase domain, Plk1$^{190-225}$ (T-loop), Bora$^{1-224}$, Bora$^{18-120}$ were expressed in *Escherichia coli* BL21 DE3 (Thermo Fisher Scientific), the fragment 10-360 of human ERK was expressed in *E. coli* BL21 DE3 pLyS RIL (Thermo Fisher Scientific). Transformed bacteria were incubated in LB (ERK, Bora$^{18-120}$) or TB

(AURKA^{T288V}, Plk1$^{1-330}$, Plk1$^{190-225}$, Bora$^{1-224}$) media at 37°C under agitation, and the cultures were shifted to 18°C at OD=0.8. Protein expression was induced by the addition of IPTG (final concentration 500 µM), and the cultures were incubated overnight at 18°C under agitation, except for Bora$^{18-120}$. In this case, the culture was shifted to 25°C and incubated for 3 hours at 25°C in the presence of IPTG.

Recombinant protein purification

6xHis-ERK$^{10-360}$ was produced essentially as described [59,83]. Briefly, bacteria expressing 6xHis-ERK10-360 were pelleted and resuspended in lysis buffer (25 mM HEPES pH 7.5, 300 mM NaCl, 20 mM Imidazole, 1 mM TCEP), supplemented with protease inhibitor cocktail (Roche) and lysed by sonication. Total extract was clarified by centrifugation (30000 g, 30 min). The resulting soluble fraction was loaded on a 5 ml Ni++ HiTrap Chelating HP (Cytiva) and eluted with an imidazole gradient on an Akta FPLC system (Cytiva). The pure fractions were collected and concentrated using an ultrafiltration centrifugal protein concentrator (MerckMilipore). The protein was finally resolved on a Hi-Load 16/600 Superdex 200 pg sizing column (Cytiva) equilibrated in 25 mM HEPES pH 7.5, 200 mM NaCl, 1 mM TCEP. The fractions containing the protein were pooled and concentrated using an ultrafiltration centrifugal protein concentrator. The purified protein was aliquoted, flash frozen, and stored at -80°C.

6xHis-TEV-Bora$^{1-224}$ WT were cloned as a TEV cleavable 6-His fusions, which leaves non-native residues (GAMDPEF) at the N-terminus after TEV digestion. Bacteria pellets were resuspended in lysis buffer (25 mM Tris pH 7.5, 150 mM NaCl, 20 mM Imidazole, 1 mM TCEP, 2 mM PMSF) and lysed by sonication at 4°C. Total extract was clarified by centrifugation (30000g, 30 min), and the resulting insoluble material was resuspended in 25 mM Tris pH 7.5, 6M Guanidine HCL, 1 mM TCEP at room temperature, sonicated, and clarified by centrifugation (30000g, 30 min). The supernatant was passed through a 0.45 µm filter and loaded on a 5 ml Ni++ Hitrap Chelating HP (Cytiva) equilibrated in 25 mM Tris pH 7.5, 6 M Guanidine HCL, 1 mM TCEP. After extensive washes, 6xHis-Bora$^{1-224}$ was eluted by 5 column volumes (CV) of elution buffer (25 mM Tris pH 7.5, 6 M Guanidine HCl, 500 mM Imidazole, 1 mM TCEP). Fractions containing the protein of interest were pooled and dialyzed against the dialysis buffer (25 mM Tris pH 7.5, 150 mM NaCl, 1 mM TCEP) for 4h to remove the guanidine HCL. 6xHis-Bora precipitated in the absence of Guanidine HCl. 6xHis-Bora$^{1-224}$ precipitated in the absence of Guanidine HCl. The content of the dialysis bag was transferred into a 50 ml conical Falcon tube and centrifuged at 4000g for 10 min. The supernatant was discarded, and the resulting pellet containing Bora was resuspended overnight by agitation in 50 ml of resuspending buffer (25 mM Tris pH 7.5, 150 mM NaCl, 2 mM TCEP). All the subsequent steps were performed at 4°C. The solubilized was clarified by centrifugation at 4000g for 10 min. The supernatant was concentrated to 5 ml using an ultrafiltration centrifugal protein concentrator (MerckMilipore) and incubated overnight with 2mg of 6xHis-TEV protease. Cleaved Bora was then loaded on a 5ml Ni++ HiTrap Chelating HP (Cytiva) to remove 6xHis-TEV and 6xHis cleaved tag. The Flow-through containing Bora was concentrated using an ultrafiltration centrifugal protein concentrator. Bora was finally resolved on a Superdex 200 16/600 GL sizing column (Cytiva) equilibrated in 25 mM Tris pH 7.5, 150 mM NaCl, 1 mM TCEP. The fractions containing Bora were pooled and concentrated using an ultrafiltration centrifugal protein concentrator. The purified protein was aliquoted, flash frozen, and stored at -80°C.

MBP-TEV-Bora$^{18-120}$ WT and mutants were cloned as a TEV-cleavable MBP fusion. Bacteria were pelleted and resuspended in lysis buffer (50 mM Tris pH 7.5, 500 mM

NaCl, 1 mM DTT), supplemented with protease inhibitor cocktail (Roche), and lysed by sonication at 4°C. Total extract was clarified by centrifugation (30000 g, 30 min). The soluble fraction was loaded on 2 x 1 ml MBP-Trap columns (Cytiva), and after washing, the protein of interest was eluted with 15 mM maltose on an AKTA pure system (Cytiva). The pure fractions were collected and injected on a HiLoad 16/600 Superdex 75 pg sizing column (Cytiva) equilibrated in 50 mM Tris pH 7.5, 500 mM NaCl, 1 mM DTT. The fractions containing Bora were pooled and concentrated using an ultrafiltration centrifugal protein concentrator. Finally, the buffer was exchanged using a G25 column for a storage buffer containing 10 mM HEPES pH 7.8, 100 mM KCl, 1 mM CaCl2, 50 mM Sucrose. The purified protein was aliquoted, flash frozen, and stored at -80°C.

6xHis-GST-TEV-AURKA$^{1\text{-}403\ T288V}$ was cloned as a TEV cleavable 6xHis-GST fusion, which leaves two non-native residues (GA) at the N-terminus after TEV digestion. Bacteria were pelleted and resuspended in lysis buffer (25 mM HEPES pH 7.5, 500 mM NaCl, 1 mM DTT) supplemented with protease inhibitor cocktail (Roche) and lysed by sonication at 4°C. Total extract was clarified by centrifugation (30000 g, 30 min). The soluble fraction was loaded onto a 1x5ml GST-Trap 4B (Cytiva) column. The TEV protease was added to the 1x5ml GST-Trap 4B (Cytiva) column with the soluble fraction loaded for 8 hours. AURKA cleaved protein was then eluted by gravity with the washing step, and the 6-His-GST-tag was eluted with the elution buffer containing 25 mM Hepes pH 7.5, 500 mM NaCl, 20 mM Glutathione, 1 mM DTT (pH with NaOH). The fractions containing cleaved AURKA were pooled, and the salt concentration was lowered to 50 mM NaCl by dilution, and the protein was loaded on 2 x 1 mL HiTrap SP HP column (Cytiva) and eluted with a salt gradient. The pure fractions were collected and concentrated using an ultrafiltration centrifugal protein concentrator (MerckMillipore). The protein was finally resolved on a HiLoad 16/600 Superdex 200 pg sizing column (Cytiva) equilibrated in 25 mM Tris pH 7.5, 150 mM NaCl, 1 mM DTT. The fractions containing the protein were pooled and concentrated using an ultrafiltration centrifugal protein concentrator. The purified protein was aliquoted, flash-frozen in liquid nitrogen, and stored at -80°C.

6xHis-GST-TEV-Plk1 Kinase Domain$^{1\text{-}330\ K82R}$ Kinase Dead, WT or mutated were cloned as a TEV cleavable 6xHis-GST fusion, which leaves seven non-native residues (GAMDPEF) at the N-terminus after TEV digestion. Bacteria were pelleted and resuspended in lysis buffer (50 mM Tris-HCl pH 7.5, 500 mM NaCl, 1 mM DTT) supplemented with protease inhibitor cocktail (Roche) and lysed by sonication at 4°C. Total extract was clarified by centrifugation (30000 g, 30 min). The soluble fraction was loaded onto a 1 ml GST-Trap FF (Cytiva) column. The TEV protease is added into the 1ml GST-Trap FF (Cytiva) column with the soluble fraction loaded during 8 hours. Plk1 cleaved protein was then eluted by gravity with the washing step, and the 6xHis-GST-tag was eluted with the elution buffer containing 100 mM Tris-HCl pH 8.8, 500 mM NaCl, 20 mM Glutathione, 1 mM DTT. The fraction containing Plk1 cleaved are pooled and the salt concentration was lowered to 50 mM NaCl by dilution and the protein was loaded on a 1mL HiTrap SP HP column (Cytiva) (Binding buffer: 50mM Tris-Hcl pH7.5, 50mM NaCl, 1mM DTT) and eluted with a salt gradient (Elution buffer: 50mM Tris-HCl pH7.5, 500mM NaCl, 1mM DTT). The pure fractions were collected and concentrated using an ultrafiltration centrifugal protein concentrator (Merck Millipore). The protein was finally resolved on a HiLoad 16/600 Superdex 75pg sizing column (Cytiva) equilibrated in 50 mM Tris pH 7.5, 150 mM NaCl, 1 mM DTT. The fractions containing the protein were pooled and concentrated using an ultrafiltration centrifugal protein concentrator. The purified protein was aliquoted, flash-frozen in liquid nitrogen, and stored at -80°C.

GST-TEV-Plk1$^{190-225}$ T-loop. Bacteria pellets were resuspended in lysis buffer (50 mM Tris-HCl pH 7.5, 500 mM NaCl, 1 mM DTT) supplemented with protease inhibitor cocktail (Roche) and lysed by sonication at 4°C. Total extract was clarified by centrifugation (30000 g, 30 min). The soluble fraction was loaded onto 1 x 5 ml GST-Trap 4B (Cytiva) column, and after washing, proteins were eluted using 20 mM Glutathione (Elution buffer: 100 mM Tris-HCl pH 8.8, 500 mM NaCl, 20 mM Glutathione, 1 mM DTT). The pure fractions were collected and concentrated using an ultrafiltration centrifugal protein concentrator (MerckMillipore). The protein was finally resolved on a HiLoad 16/600 Superdex 200 pg sizing column (Cytiva) equilibrated in 25 mM Tris pH 7.5, 150 mM NaCl, 1 mM DTT. The fractions containing the protein were pooled and concentrated using an ultrafiltration centrifugal protein concentrator. The purified protein was aliquoted, flash-frozen in liquid nitrogen, and stored at -80°C.

The concentration of all the purified recombinant proteins was determined using Bradford reagent (Thermo Fisher Scientific).

Biochemistry

ADP Glo™ assay: The ATPase activity of recombinant AURKA was evaluated using the ADP-Glo assay Kinase kit (Promega). Bora$^{1-224}$ or pBora$^{1-224}$ was titrated into 10 nM of AURKA^{WT} or AURKA^{T288V} in a buffer containing 40 mM Tris pH7.5, 150 mM NaCl, 10 mM MgCl2, 1 mM DTT, 0.1 mg/ml BSA, and 0.01% Brij 35. The final reaction volume was 20 µL. When 100 µM Kemptide (LRRASLG, Cedarlane) was present in the reaction mix, the Aurka A concentration was reduced to 2 nM. Reactions were initiated by the addition of 10 µM of ATP and incubated at room temperature for 60 minutes. Reactions were terminated by transferring 10 µL of the reaction mix to a 384 well white plate (Lumitrec 200, VWR) and adding 10 µL of ADP-Glo™ Reagent (Promega). After a 40 min incubation, 20 µL of kinase detection reagent (Promega) was added and allowed to incubate for an additional 30 minutes. Luminescence was measured on a Biotek Synergy Neo plate reader (BioTek) using a 1 second integration time. Results were plotted in GraphPad Prism V8.4.2 using a one-site total binding curve fitting analysis.

Fluorescence Polarization Binding assay: FITC-Tpx2$^{1-43}$ and unlabeled Tpx2$^{1-43}$ were synthesized by Proteogenix (Schiltigheim, France). Unlabeled proteins and FITC-Tpx2$^{1-43}$ were mixed in FP buffer (25 mM HEPES pH 7.5, 50 mM NaCl, 10 mM $MgCl_2$, 0.1 mg/ml BSA (Sigma), 0.01% Brij, 3 mM ADP(Sigma), 2 mM DTT) in a 384-well flat bottom black plate (Corning 3573) at a final volume of 25 µL. For Kd extraction, FITC-Tpx2$^{1-43}$ probe was kept at 5 nM throughout experiments, and each analyzed protein was added to the concentrations indicated in each figure. Each data point was derived from a technical duplicate and each binding curve was performed in triplicate. For the competitive displacement assay, FITC-Tpx2$^{1-43}$ (5 nM) and AURKA protein concentrations (35 nM) were kept constant throughout experiments, and unlabeled competitor (either Bora or Tpx2) were added to final concentrations indicated in each figure. Fluorescence polarization was measured on a BioTek Synergy Neo plate reader (BioTek) using Gen5 v2.05 software with excitation and absorbance at 485/528 nm, respectively. Binding graphs and the derived binding constants were generated using GraphPad Prism v8.1.2 and v8.3 (GraphPad). Error bars on binding graphs represent deviation between duplicate data points. Kd and IC50 SD values represent deviation between values obtained from three binding experiments.

Kinase assays: The assay was performed in two steps. Step 1 consisted of the phosphorylation of 2 µM of Bora fragments by Erk (molar ratio 5:1) in 10 µL of kinase buffer (25 mM HEPES pH 7.5, 150 mM NaCl, 20 mM $MgCl_2$, 1 mM DTT, 200 µM ATP)

incubated for 1h at 30°C. Step 2 consisted of the phosphorylation of 200 nM of Plk1^{K82R} by AURKA (molar ratio 1:1) in the presence of 400 nM of Bora from step 1 in 30 µL of kinase buffer, incubated 30 min at 30°C.

SDS-PAGE, Western-Blot experiments:
Samples were electrophoresed on SDS-PAGE (12% Acrylamide home-made gel) and electro-transferred to nitrocellulose membrane (0.45 µm NC, 10600002; Amersham Protran). Next, Western blots were probed with primary and appropriate secondary antibodies. Western blots were performed following standard procedures.
Antibodies used in this study are listed below. HRP-conjugated anti-rabbit and anti-mouse antibodies (Sigma-Aldrich) were used at 1:5000, and the signal was detected by chemiluminescence (Millipore) with ChemiDoc MP Imaging System (Bio-Rad).
Quantification of Western blot images was performed using ImageLab software (Bio-Rad), with adjusted values obtained by normalizing the pT210/Plk1 or pS10H3/H3 signal ratio.

Antibodies:
The antibodies used in this study are the following: mouse anti-Bora 1/400 (Santa-Cruz Cat#sc-393741), rabbit anti-AURKA 1/2000 (Cell Signaling Technologies Cat#91590), rabbit anti-Phospho-Plk1 (Thr210) 1/1000 (Cell Signaling, Technologies Cat#5472), rabbit anti-human Plk1 1/2000 (Bethyl Cat#A300-250A), rabbit anti-GST 1/1000 (Cell Signaling Cat#2622), rabbit anti-Phospho-Histone H3 (Ser10) 1/1000 (Cell Signaling Cat#3377S), rabbit anti-Histone H3 1/1000 (Abcam, Cat#AB1791), mouse anti-MBP 1/5000 (NEB biolabs cat#E8032S). Rabbit Anti-human Greatwall 1/1000 [84], rabbit anti-Xenopus Plx1 1/1000 [60], rabbit anti-Phospho-Cdc2 (Tyr15) 1/1000 (Cell Signaling Technologies Cat#9111),

Interphase Xenopus Egg Extracts:
Preparation of Xenopus extracts:
Interphase egg extracts were obtained from dejellied unfertilised eggs transferred into MMR solution (1.25 mM HEPES-NaOH pH7.7, 25 mM NaCl, 0.5 mM KCl, 0.25 mM MgCl2, 0.025 mM NaEGTA,) supplemented with Ca2+ ionophore addition (final concentration 2 µg/ml) and 35 minutes later recovered and rinsed with XB buffer (10 mM HEPES at pH 7.7, 100 mM KCl, 0.1 mM MgCl2, 50 mM Sucrose, 5 mM NaEGTA,) and subsequently centrifuged twice for 20 minutes at 10 000g and the cytoplasmic fractions recovered in aliquots of 70 µL [85]. 1 µL of Interphase egg extracts was loaded on a polyacrylamide gel and transferred onto N Immobilon-P membranes. Membranes were blocked either with 5% milk TBST for detection of hs Gwl, xl Gwl, Plx1, and hs Bora proteins, or with 2% BSA TBST for detection of pPlx1 and P-Y-15 CDK1 phospho-proteins. Rabbit peroxidase (HRP)-conjugated secondary antibodies were used. Proteins reacting with the antibodies were detected using ECL reaction (MerckMillipore).

Immunodepletion Xenopus extracts:
To deplete Xenopus egg extracts, immunoprecipitations were carried out for 20 minutes at room temperature using 2 µg of affinity-purified antibodies immobilized on 20 µl protein G-Dynabeads (Dynal) and 20 µl of Xenopus egg extracts. When supernatant was used, beads were removed by magnetic racks, and supernatants recovered. Two consecutive immunoprecipitations were performed to completely remove endogenous Bora protein~~s~~. Bora immunoprecipitation was performed using antibodies raised against GST-full length Xenopus Bora, whereas Western blot was performed with antibodies against Xenopus-Nter-Bora [60].

Protein sequence alignment:
Sequences were aligned using ClustalW [86] and visualized with Jalview [87].

AlphaFold3 Modelling
Protein sequences were downloaded from Uniprot. We accessed AlphaFold 3 from its virtual server (https://alphafoldserver.com/welcome) to run pairwise predictions with 5 models per prediction. Predicted structures were visualized with ChimeraX-1.8 [88,89].

Data and Code availability
AlphaFold3 model: Bora•AURKA•Plk1^{KDom} complex:
>AURKA$^{126-403}$ (278 aa)
RQWALEDFEIGRPLGKGKFGNVYLAREKQSKFILALKVLFKAQLEKAGVEHQLRREVEIQSHLRHPNIL
RLYGYFHDATRVYLILEYAPLGTVYRELQKLSKFDEQRTATYITELANALSYCHSKRVIHRDIKPENLLLG
SAGELKIADFGWSVHAPSSRRTTLCGTLDYLPPEMIEGRMHDEKVDLWSLGVLCYEFLVGKPPFEANT
YQETYKRISRVEFTFPDFVTEGARDLISRLLKHNPSQRPMLREVLEHPWITANSSKPSNCQNKESASKQ
S

>Bora$^{18-116}$ (99 aa)
RIPVLNPFESPSDYSNLHEQTLASPSVFKSTKLPTPGKFRWSIDQLAVINPVEIDPEDIHRQALYLSHSRI
DKDVEDKRQKAIEEFFTKDVIVPSPWTD

> Plk1$^{KDom\ 1-332}$ (332 aa)
MSAAVTAGKLARAPADPGKAGVPGVAAPGAPAAAPPAKEIPEVLVDPRSRRRYVRGRFLGKGGFAKC
FEISDADTKEVFAGKIVPKSLLLKPHQREKMSMEISIHRSLAHQHVVGFHGFFEDNDFVFVVLELCRRRS
LLELHKRRKALTEPEARYYLRQIVLGCQYLHRNRVIHRDLKLGNLFLNEDLEVKIGDFGLATKVEYDGER
KKTLCGTPNYIAPEVLSKKGHSFEVDVWSIGCIMYTLLVGKPPFETSCLKETYLRIKKNEYSIPKHINPVA
ASLIQKMLQTDPTARPTINELLNDEFFTSGYIPARLPITCLTIPPRFSIAPSSL

Atomic structures:
AURKA•Tpx2
PDB: 1OL5 [http://DOI:10.2210/pdb1OL5/pdb] [44,64]

AURKA•Cep192
PDB: 8PR7 [https://doi.org/10.2210/pdb8PR7/pdb] [65],
PBD: 8GUW [https://doi.org/10.2210/pdb8GUW/pdb] [66]

AURKA•TACC3
PDB: 5ODT [https://doi.org/10.2210/pdb5ODT/pdb] [67],

Statistics and Reproducibility:
Except when specifically indicated, all experiments presented in this manuscript have been repeated at least three times

Data Availability statement:
The authors declare that the data supporting the findings of this study are available within the paper and its supplementary information files. Source data are provided with this paper. Uncropped gels and blots are presented in this source data file.

Authors contributions
Conceptualization, AP, TL, FS and LP
Methodology, AP, PO, SO, LVH, NT, BON, NJ, CBC, TL
Investigation, AP, PO, SO, LVH, NT, CBC, TL
Writing – Original Draft, LP
Writing – Review & Editing, AP, NJ, BON, TL, FS, and LP
Supervision: LP

Funding acquisition, TL, FS, and LP

Competing Interests: The authors declare no competing interests.

References

1. Champion, L., Linder, M. I. & Kutay, U. Cellular Reorganization during Mitotic Entry. *Trends Cell Biol* **27**, 26-41 (2017).
2. Glover, D. M., Leibowitz, M. H., McLean, D. A. & Parry, H. Mutations in aurora prevent centrosome separation leading to the formation of monopolar spindles. *Cell* **81**, 95-105 (1995).
3. Llamazares, S. et al. polo encodes a protein kinase homolog required for mitosis in Drosophila. *Genes Dev* **5**, 2153-2165 (1991).
4. Sunkel, C. E. & Glover, D. M. polo, a mitotic mutant of Drosophila displaying abnormal spindle poles. *J Cell Sci* **89**, 25-38 (1988).
5. Nigg, E. A. Mitotic kinases as regulators of cell division and its checkpoints. *Nat Rev Mol Cell Biol* **2**, 21-32 (2001).
6. Dephoure, N. et al. A quantitative atlas of mitotic phosphorylation. *Proc Natl Acad Sci U S A* **105**, 10762-10767 (2008).
7. Lindqvist, A., Rodriguez-Bravo, V. & Medema, R. H. The decision to enter mitosis: feedback and redundancy in the mitotic entry network. *J Cell Biol* **185**, 193-202 (2009).
8. Zitouni, S., Nabais, C., Jana, S. C., Guerrero, A. & Bettencourt-Dias, M. Polo-like kinases: structural variations lead to multiple functions. *Nat Rev Mol Cell Biol* **15**, 433-452 (2014).
9. Joukov, V. & De Nicolo, A. Aurora-PLK1 cascades as key signaling modules in the regulation of mitosis. *Sci Signal* **11**, (2018).
10. Seki, A., Coppinger, J. A., Jang, C. Y., Yates, J. R. & Fang, G. Bora and the kinase Aurora a cooperatively activate the kinase Plk1 and control mitotic entry. *Science* **320**, 1655-1658 (2008).
11. Aspinall, C. F., Zheleva, D., Tighe, A. & Taylor, S. S. Mitotic entry: Non-genetic heterogeneity exposes the requirement for Plk1. *Oncotarget* **6**, 36472-36488 (2015).
12. Gheghiani, L., Loew, D., Lombard, B., Mansfeld, J. & Gavet, O. PLK1 Activation in Late G2 Sets Up Commitment to Mitosis. *Cell Rep* **19**, 2060-2073 (2017).
13. Gobran, M. et al. PLK1 inhibition delays mitotic entry revealing changes to the phosphoproteome of mammalian cells early in division. *EMBO J* **44**, 1891-1920 (2025).
14. Lane, H. A. & Nigg, E. A. Antibody microinjection reveals an essential role for human polo-like kinase 1 (Plk1) in the functional maturation of mitotic centrosomes. *J Cell Biol* **135**, 1701-1713 (1996).
15. Sumara, I. et al. The dissociation of cohesin from chromosomes in prophase is regulated by Polo-like kinase. *Mol Cell* **9**, 515-525 (2002).
16. Abe, S. et al. The initial phase of chromosome condensation requires Cdk1-mediated phosphorylation of the CAP-D3 subunit of condensin II. *Genes Dev* **25**, 863-874 (2011).
17. Linder, M. I. et al. Mitotic Disassembly of Nuclear Pore Complexes Involves CDK1- and PLK1-Mediated Phosphorylation of Key Interconnecting Nucleoporins. *Dev Cell* **43**, 141-156.e7 (2017).
18. Martino, L. et al. Channel Nucleoporins Recruit PLK-1 to Nuclear Pore Complexes to Direct Nuclear Envelope Breakdown in C. elegans. *Dev Cell* **43**, 157-171.e7 (2017).
19. Sumara, I. et al. Roles of polo-like kinase 1 in the assembly of functional mitotic spindles. *Curr Biol* **14**, 1712-1722 (2004).

20. Elowe, S., Hümmer, S., Uldschmid, A., Li, X. & Nigg, E. A. Tension-sensitive Plk1 phosphorylation on BubR1 regulates the stability of kinetochore microtubule interactions. *Genes Dev* **21**, 2205-2219 (2007).
21. Petronczki, M., Glotzer, M., Kraut, N. & Peters, J. M. Polo-like kinase 1 triggers the initiation of cytokinesis in human cells by promoting recruitment of the RhoGEF Ect2 to the central spindle. *Dev Cell* **12**, 713-725 (2007).
22. Burkard, M. E. et al. Chemical genetics reveals the requirement for Polo-like kinase 1 activity in positioning RhoA and triggering cytokinesis in human cells. *Proc Natl Acad Sci U S A* **104**, 4383-4388 (2007).
23. Archambault, V. & Glover, D. M. Polo-like kinases: conservation and divergence in their functions and regulation. *Nat Rev Mol Cell Biol* **10**, 265-275 (2009).
24. Saurin, A. T. Kinase and Phosphatase Cross-Talk at the Kinetochore. *Front Cell Dev Biol* **6**, 62 (2018).
25. Combes, G., Alharbi, I., Braga, L. G. & Elowe, S. Playing polo during mitosis: PLK1 takes the lead. *Oncogene* **36**, 4819-4827 (2017).
26. Pintard, L. & Archambault, V. A unified view of spatio-temporal control of mitotic entry: Polo kinase as the key. *Open Biol* **8**, (2018).
27. Hirota, T. et al. Aurora-A and an interacting activator, the LIM protein Ajuba, are required for mitotic commitment in human cells. *Cell* **114**, 585-598 (2003).
28. Hannak, E., Kirkham, M., Hyman, A. A. & Oegema, K. Aurora-A kinase is required for centrosome maturation in Caenorhabditis elegans. *J Cell Biol* **155**, 1109-1116 (2001).
29. Giet, R. et al. Drosophila Aurora A kinase is required to localize D-TACC to centrosomes and to regulate astral microtubules. *J Cell Biol* **156**, 437-451 (2002).
30. Berdnik, D. & Knoblich, J. A. Drosophila Aurora-A is required for centrosome maturation and actin-dependent asymmetric protein localization during mitosis. *Curr Biol* **12**, 640-647 (2002).
31. Nikonova, A. S., Astsaturov, I., Serebriiskii, I. G., Dunbrack, R. L. & Golemis, E. A. Aurora A kinase (AURKA) in normal and pathological cell division. *Cell Mol Life Sci* **70**, 661-687 (2013).
32. Magnaghi-Jaulin, L., Eot-Houllier, G., Gallaud, E. & Giet, R. Aurora A Protein Kinase: To the Centrosome and Beyond. *Biomolecules* **9**, (2019).
33. Endicott, J. A., Noble, M. E. & Johnson, L. N. The structural basis for control of eukaryotic protein kinases. *Annu Rev Biochem* **81**, 587-613 (2012).
34. Bayliss, R., Fry, A., Haq, T. & Yeoh, S. On the molecular mechanisms of mitotic kinase activation. *Open Biol* **2**, 120136 (2012).
35. Huse, M. & Kuriyan, J. The conformational plasticity of protein kinases. *Cell* **109**, 275-282 (2002).
36. Johnson, L. N. & Lewis, R. J. Structural basis for control by phosphorylation. *Chem Rev* **101**, 2209-2242 (2001).
37. Welburn, J. P. I. & Jeyaprakash, A. A. Mechanisms of Mitotic Kinase Regulation: A Structural Perspective. *Front Cell Dev Biol* **6**, 6 (2018).
38. Beenstock, J., Mooshayef, N. & Engelberg, D. How Do Protein Kinases Take a Selfie (Autophosphorylate). *Trends Biochem Sci* **41**, 938-953 (2016).
39. Kelm, O., Wind, M., Lehmann, W. D. & Nigg, E. A. Cell cycle-regulated phosphorylation of the Xenopus polo-like kinase Plx1. *J Biol Chem* **277**, 25247-25256 (2002).
40. Jang, Y. J., Ma, S., Terada, Y. & Erikson, R. L. Phosphorylation of threonine 210 and the role of serine 137 in the regulation of mammalian polo-like kinase. *J Biol Chem* **277**, 44115-44120 (2002).
41. Macurek, L. et al. Polo-like kinase-1 is activated by aurora A to promote checkpoint recovery. *Nature* **455**, 119-123 (2008).

42. Littlepage, L. E. et al. Identification of phosphorylated residues that affect the activity of the mitotic kinase Aurora-A. *Proc Natl Acad Sci U S A* **99**, 15440-15445 (2002).
43. Eyers, P. A., Erikson, E., Chen, L. G. & Maller, J. L. A novel mechanism for activation of the protein kinase Aurora A. *Curr Biol* **13**, 691-697 (2003).
44. Bayliss, R., Sardon, T., Vernos, I. & Conti, E. Structural basis of Aurora-A activation by TPX2 at the mitotic spindle. *Mol Cell* **12**, 851-862 (2003).
45. Zorba, A. et al. Molecular mechanism of Aurora A kinase autophosphorylation and its allosteric activation by TPX2. *Elife* **3**, e02667 (2014).
46. Walter, A. O., Seghezzi, W., Korver, W., Sheung, J. & Lees, E. The mitotic serine/threonine kinase Aurora2/AIK is regulated by phosphorylation and degradation. *Oncogene* **19**, 4906-4916 (2000).
47. Katayama, H., Zhou, H., Li, Q., Tatsuka, M. & Sen, S. Interaction and feedback regulation between STK15/BTAK/Aurora-A kinase and protein phosphatase 1 through mitotic cell division cycle. *J Biol Chem* **276**, 46219-46224 (2001).
48. Kang, Q., Srividhya, J., Ipe, J. & Pomerening, J. R. Evidence toward a dual phosphatase mechanism that restricts Aurora A (Thr-295) phosphorylation during the early embryonic cell cycle. *J Biol Chem* **289**, 17480-17496 (2014).
49. Levinson, N. M. The multifaceted allosteric regulation of Aurora kinase A. *Biochem J* **475**, 2025-2042 (2018).
50. Tavernier, N., Sicheri, F. & Pintard, L. Aurora A kinase activation: Different means to different ends. *J Cell Biol* **220**, (2021).
51. Kufer, T. A. et al. Human TPX2 is required for targeting Aurora-A kinase to the spindle. *J Cell Biol* **158**, 617-623 (2002).
52. Tsai, M. Y. et al. A Ran signalling pathway mediated by the mitotic kinase Aurora A in spindle assembly. *Nat Cell Biol* **5**, 242-248 (2003).
53. Dodson, C. A. & Bayliss, R. Activation of Aurora-A kinase by protein partner binding and phosphorylation are independent and synergistic. *J Biol Chem* **287**, 1150-1157 (2012).
54. Burgess, S. G. & Bayliss, R. The structure of C290A:C393A Aurora A provides structural insights into kinase regulation. *Acta Crystallogr F Struct Biol Commun* **71**, 315-319 (2015).
55. Cyphers, S., Ruff, E. F., Behr, J. M., Chodera, J. D. & Levinson, N. M. A water-mediated allosteric network governs activation of Aurora kinase A. *Nat Chem Biol* **13**, 402-408 (2017).
56. Hutterer, A. et al. Mitotic activation of the kinase Aurora-A requires its binding partner Bora. *Dev Cell* **11**, 147-157 (2006).
57. Thomas, Y. et al. Cdk1 Phosphorylates SPAT-1/Bora to Promote Plk1 Activation in C. elegans and Human Cells. *Cell Rep* **15**, 510-518 (2016).
58. Tavernier, N. et al. Cdk1 phosphorylates SPAT-1/Bora to trigger PLK-1 activation and drive mitotic entry in C. elegans embryos. *J Cell Biol* **208**, 661-669 (2015).
59. Tavernier, N. et al. Bora phosphorylation substitutes in trans for T-loop phosphorylation in Aurora A to promote mitotic entry. *Nat Commun* **12**, 1899 (2021).
60. Vigneron, S. et al. Cyclin A-cdk1-Dependent Phosphorylation of Bora Is the Triggering Factor Promoting Mitotic Entry. *Dev Cell* **45**, 637-650.e7 (2018).
61. Silva Cascales, H. et al. Cyclin A2 localises in the cytoplasm at the S/G2 transition to activate PLK1. *Life Sci Alliance* **4**, (2021).
62. Zegzouti, H., Zdanovskaia, M., Hsiao, K. & Goueli, S. A. ADP-Glo: A Bioluminescent and homogeneous ADP monitoring assay for kinases. *Assay Drug Dev Technol* **7**, 560-572 (2009).

63. Crosio, C. et al. Mitotic phosphorylation of histone H3: spatio-temporal regulation by mammalian Aurora kinases. *Mol Cell Biol* **22**, 874-885 (2002).
64. McIntyre, P. J. et al. Characterization of Three Druggable Hot-Spots in the Aurora-A/TPX2 Interaction Using Biochemical, Biophysical, and Fragment-Based Approaches. *ACS Chem Biol* **12**, 2906-2914 (2017).
65. Holder, J. et al. CEP192 localises mitotic Aurora-A activity by priming its interaction with TPX2. *EMBO J* (2024).
66. Park, J. G. et al. Structural basis for CEP192-mediated regulation of centrosomal AURKA. *Sci Adv* **9**, eadf8582 (2023).
67. Burgess, S. G. et al. Mitotic spindle association of TACC3 requires Aurora-A-dependent stabilization of a cryptic α-helix. *EMBO J* **37**, (2018).
68. Joukov, V., De Nicolo, A., Rodriguez, A., Walter, J. C. & Livingston, D. M. Centrosomal protein of 192 kDa (Cep192) promotes centrosome-driven spindle assembly by engaging in organelle-specific Aurora A activation. *Proc Natl Acad Sci U S A* **107**, 21022-21027 (2010).
69. Chan, E. H., Santamaria, A., Sillje, H. H. & Nigg, E. A. Plk1 regulates mitotic Aurora A function through betaTrCP-dependent degradation of hBora. *Chromosoma* **117**, 457-469 (2008).
70. Rogerson, D. T. et al. Efficient genetic encoding of phosphoserine and its nonhydrolyzable analog. *Nat Chem Biol* **11**, 496-503 (2015).
71. Qin, X. & Liu, T. Recent Advances in Genetic Code Expansion Techniques for Protein Phosphorylation Studies. *J Mol Biol* **434**, 167406 (2022).
72. Zhu, P., Mehl, R. A. & Cooley, R. B. Site-specific Incorporation of Phosphoserine into Recombinant Proteins in Escherichia coli. *Bio Protoc* **12**, e4541 (2022).
73. Roumbo, L. et al. The MAST kinase KIN-4 carries out mitotic entry functions of Greatwall in C. elegans. *EMBO J* **44**, 1943-1974 (2025).
74. Keskitalo, S. et al. The non-catalytic ε DNA polymerase subunit is an NPF motif recognition protein. *bioRxiv* 2025.03.17.643635 (2025).
75. Deretic, J., Kerr, A. & Welburn, J. P. I. A rapid computational approach identifies SPICE1 as an Aurora kinase substrate. *Mol Biol Cell* **30**, 312-323 (2019).
76. Lössl, P. et al. Deciphering the Interplay among Multisite Phosphorylation, Interaction Dynamics, and Conformational Transitions in a Tripartite Protein System. *ACS Cent Sci* **2**, 445-455 (2016).
77. Seki, A. et al. Plk1- and beta-TrCP-dependent degradation of Bora controls mitotic progression. *J Cell Biol* **181**, 65-78 (2008).
78. Vigneron, S. et al. Greatwall maintains mitosis through regulation of PP2A. *EMBO J* **28**, 2786-2793 (2009).
79. Bruinsma, W. et al. Inhibition of Polo-like kinase 1 during the DNA damage response is mediated through loss of Aurora A recruitment by Bora. *Oncogene* (2016).
80. Parrilla, A. et al. Aurora Borealis (Bora), Which Promotes Plk1 Activation by Aurora A, Has an Oncogenic Role in Ovarian Cancer. *Cancers (Basel)* **12**, (2020).
81. Cheng, S. et al. BORA regulates cell proliferation and migration in bladder cancer. *Cancer Cell Int* **20**, 290 (2020).
82. Barber, M. et al. BORA overexpression promotes epithelial-mesenchymal transition and metastasis in ovarian cancer: Unveiling a novel therapeutic target for advanced disease. *Clin Transl Med* **15**, e70285 (2025).
83. Khokhlatchev, A. et al. Reconstitution of mitogen-activated protein kinase phosphorylation cascades in bacteria. Efficient synthesis of active protein kinases. *J Biol Chem* **272**, 11057-11062 (1997).

84. Burgess, A. et al. Loss of human Greatwall results in G2 arrest and multiple mitotic defects due to deregulation of the cyclin B-Cdc2/PP2A balance. *Proc Natl Acad Sci U S A* **107**, 12564-12569 (2010).
85. Lorca, T. et al. Constant regulation of both the MPF amplification loop and the Greatwall-PP2A pathway is required for metaphase II arrest and correct entry into the first embryonic cell cycle. *J Cell Sci* **123**, 2281-2291 (2010).
86. Larkin, M. A. et al. Clustal W and Clustal X version 2.0. *Bioinformatics* **23**, 2947-2948 (2007).
87. Waterhouse, A. M., Procter, J. B., Martin, D. M., Clamp, M. & Barton, G. J. Jalview Version 2--a multiple sequence alignment editor and analysis workbench. *Bioinformatics* **25**, 1189-1191 (2009).
88. Pettersen, E. F. et al. UCSF ChimeraX: Structure visualization for researchers, educators, and developers. *Protein Sci* **30**, 70-82 (2021).
89. Meng, E. C. et al. UCSF ChimeraX: Tools for structure building and analysis. *Protein Sci* **32**, e4792 (2023).

Figure legends:

Figure 1: **A phosphorylated Tpx2-Bora chimera potentiates the kinase activity of non-phosphorylated AURKA.**

A- Schematic of AURKA activation mechanisms during mitotic entry (left panel) and spindle assembly (right panel) by its allosteric activators phospho-Bora and Tpx2, respectively. In the G2 phase of the cell cycle, AURKA is maintained dephosphorylated on the T-loop (T288) by counteracting phosphatases. During mitotic entry, Cyclin A-Cdk1 phosphorylates Bora, which then binds and activates AURKA. Phospho-Bora preferentially binds unphosphorylated AURKA. Activated by pBora, AURKA phosphorylates the Plk1 T-loop (T210) to activate the kinase and trigger mitotic entry. Then, during mitosis, Tpx2, through its first 43 amino acids, recruits and activates phosphorylated AURKA (pT288) at the microtubules to promote mitotic spindle assembly.

B- Domain architecture of *Homo sapiens* Bora (orange, left panel) and Tpx2 (blue, right panel) with the minimal fragments required for AURKA activation highlighted in dark orange ($Bora^{18-120}$) and dark blue ($Tpx2^{1-43}$). Important sequence elements identified in these regions are indicated, including the aromatic anchors in the M1 and M2 motifs of Bora and Tpx2, as well as the phosphorylatable PSP motif (M3) (green) of Bora, located just downstream of the M2 motif. Based on these sequences, we engineered a phosphorylated Tpx2-Bora fusion (phosphopeptide MK51, left panel) that reconstitutes the regulatory properties of both proteins. We also engineered a minimal Bora construct (phosphopeptide GK51, right panel) by directly fusing the putative M1 motif to the M2 and M3 motifs via a Glycine linker.

C- Competitive binding assay where fluorescein-labeled $Tpx2^{1-43}$ polypeptide, in complex with $AURKA^{T288V}$, is displaced by increasing amounts of competitor (cold $Tpx2^{1-43}$, $pBora^{1-224}$, pBora fusion, and pTxp2-Bora chimera) and monitored through fluorescence polarization signals. The displayed data points and the half maximal inhibitory concentration (IC_{50}) value represent the average fluorescence polarization for each reaction condition, with standard deviations of the mean as error bars (N=3 independent experiments, each performed with n=3 independent experimental samples). ND: not determined.

D- Activation of $AURKA^{T288V}$ ATPase activity by different activators as assessed using the ADP Glo assay with Kemptide substrate. Displayed data points and EC_{50} values represent the average luminescence for each reaction condition with standard

deviations of the mean as error bars (*N*=3 independent experiments, each performed with *n*=3 independent experiment samples). RLU: relative light unit.

Figure 2: The pTpx2-Bora chimera lacks determinants necessary to direct AURKA^{T288V} kinase activity toward the Plk1 kinase domain.

A- Schematic of the two-step *in vitro* reconstitution of Histone H3 phosphorylation on S10 by AURKA^{T288V} and pBora$^{1-224}$ or the pTpx2-Bora chimera. In step 1, Bora$^{1-224}$ phosphorylated by ERK (noted pBora) or the pTpx2-Bora chimera is incubated with AURKA^{T288V} for 15 minutes. In step 2, the reaction mix from step 1 is incubated in the presence of Mg/ATP with Histone H3 for 5, 10, 20, 30, and 60 minutes. Samples were then analyzed by Western blot. Blots were probed with antibodies to Bora, phospho-S10 Histone H3, or pan Histone H3, and AURKA (from top to bottom). Note that during step 2, pBora$^{1-224}$ itself is phosphorylated by activated AURKA^{T288V} during the reaction, which is manifested by a mobility shift in SDS-PAGE, as reported previously [59]. ppBora thus denotes Bora phosphorylated by ERK during step 1 and by activated AURKA during step 2 in this and other Figures.

B- Schematic of the two-step *in vitro* reconstitution of T-loop phosphorylation on T210 of Plk1 (pT210) by AURKA^{T288V} and pBora$^{1-224}$ or the pTpx2-Bora chimera. In step 1, pBora$^{1-224}$ or the pTpx2-Bora chimera is incubated with AURKA^{T288V} for 15 minutes. In step 2, the reaction mix in step 1 is incubated in the presence of Mg/ATP with Plk1 kinase domain catalytically dead mutant (Plk1^{K82R}) for 5, 10, 20, 30, and 60 minutes. Samples were then analyzed by Western blot. Blots were probed with antibodies to Bora, phospho-T210 Plk1, or pan Plk1, and AURKA (from top to bottom).

C- Same experiment as in panel B, except that AURKA^{T288V} activated by pBora$^{1-224}$ or the pTpx2-Bora chimera is incubated with the isolated Plk1 T-loop fused to GST as substrate. Blots were probed with antibodies to Bora, phospho-T210 Plk1, GST, and AURKA (from top to bottom)

D- Side-by-side comparison of the two-step *in vitro* reconstitution of T-loop phosphorylation on T210 of Plk1 (pT210) by AURKA^{T288V} and pBora$^{1-224}$ or the pTpx2-Bora chimera when the Plk1 kinase domain or only the isolated T-loop is used as a substrate. In step 1, pBora$^{1-224}$ or the pTpx2-Bora chimera is incubated with AURKA^{T288V} for 15 minutes. In step 2, the reaction mix in step 1 is incubated in the presence of Mg/ATP with Plk1 kinase domain catalytically dead mutant (Plk1^{K82R}) or the isolated Plk1 T-loop for 30 and 60 minutes. Samples were then analyzed by Western blot. Blots

were probed with antibodies to Bora, phospho-T210 Plk1, pan Plk1, or GST, and AURKA (from top to bottom).

E- Schematics summarizing the main results. The pTpx2-Bora chimera and pBora$^{1-224}$ can similarly activate AURKA^{T288V} toward Histone H3 (red arrows). However, in sharp contrast to pBora$^{1-224}$, the pTpx2-Bora chimera is unable to activate AURKA^{T288V} toward the Plk1 T-loop embedded in the kinase domain (crossed arrow). Both the pTpx2-Bora chimera and pBora$^{1-224}$ can stimulate AURKA ^{T288V} activity towards the isolated T-loop, but with poor efficacy (thin red arrows).

Figure 3: pBora$^{18-120}$ binding to AURKA predicted by AlphaFold compared to the structure of the Tpx2$^{1-43}$ •AURKA complex.

A- Multiple protein sequence alignments of the minimally active Bora fragment from different species, including *Homo sapiens (H. s)* [accession number: Q6PGQ7], *Danio Rerio (D. r)* [Q5U3U6], *Rattus norvegicus (R. n)* [Q5M864], *Mus musculus (M. m)* [Q8BS90], *Drosophila melanogaster (D. m)* [Q9VVR2], *Xenopus laevis (X. l)* [Q6DJL7], *Caenorhabditis elegans (C. e)* [H2FLK2], *Monodelphis domestica (M. d)* [F6XNR5], *Pongo abelii (P. a)* [H2NK15], *Ictidomys tridecemlinea (I. t)* [I3MI81], *Oryctolagus cuniculus (O. c)* [G1TPL0], *Felis catus (F. c)* [M3WCM8], *Sus scrofa (S. s)* [I3LG24], *Macaca mulatta (M. m)* [F7HH76], *Ficedula albicollis (F. a)* [U3JE63], *Taeniopygia guttata (T. g)* [H0ZQH5], *Meleagris gallopavo (M. g)* [G1NQ02]. Sequences were aligned using ClustalW and visualized with Jalview. The darker blue color indicates higher similarity and identity. The M1, M2, M3, and Bora-specific motifs (BSM) are surrounded by a rectangle.

B- Structure of Tpx2$^{1-43}$ (blue) bound to AURKA (grey) [44]. The critical aromatic residues of Tpx2$^{1-43}$ engaging the Y pocket (yellow), the F pocket (green), and the W pocket (magenta) are indicated. The schematic at the bottom shows the aromatic residues in the M1 and M2 motifs and the relative orientation of these two motifs when bound to AURKA. The dashed line shows the disordered linker region between the two motifs. The arrowheads show the orientation (N-terminal to C-terminal) of the Tpx2 fragment when bound to AURKA.

C- Zoom in view of the activation segment region of AURKA (grey) bound to Tpx2$^{1-43}$ (blue). The phosphorylated residue of the T-loop (pT288, in green) is coordinate by direct contact with R180, R255, and R286 (light blue).

D- Side and top view of the AlphaFold3 model of phospho-Bora$^{18-116}$ (orange) binding to the AURKA kinase domain (grey). AURKA is oriented as in **Fig. 3B** for direct

comparison. Aromatic and hydrophobic residues of Bora binding the Y (yellow), F (green), and W (magenta) pockets of AURKA are indicated, as well as the solvent-exposed aromatic and hydrophobic residues of Bora at the back of AURKA (red arrows).
E- Zoom in view of the activation segment region of AURKA (grey) bound to pBora (orange) in an AlphaFold3 model. The helical M2 motif, anchored via F103 and F104 residues binding to the W pocket, projects the essential phosphosite S112 (in red) into the arginine pockets composed of R180, R255, and R286 (light blue).
F- Rear view of the AlphaFold3 model of phospho-Bora$^{18-116}$ (orange) binding to the AURKA kinase domain (grey), showing the hydrophobic residues I60, I71, and I76 binding AURKA pockets while F56, W58, and I66 residues are solvent exposed (red arrows).

Figure 4: **Mitotic Kinases Activation in *E. coli* (MITOKINAC): a streamlined method that reconstitutes phospho-Bora-dependent AURKA^{T288V} activation toward the Plk1 T-loop in *E. coli.***
A- Schematic of MITOKINAC: *E. coli* BL21 are transformed with three plasmids containing different replication origins, antibiotic resistance, and expressing i) the active ERK kinase (MAPKK constitutively activated S118E, S222D, which phosphorylates and activates the MAPK ERK), ii) Bora$^{1-224}$ and AURKA^{T288V} expressed from the same plasmid, and iii) the Plk1 kinase domain (kinase-dead K82R but phosphorylable on the T-loop (T210)) or the isolated T-loop fused to GST as substrates. After co-transformation, culture, and protein induction with IPTG, Plk1 T-loop phosphorylation (T210) is monitored by Western blot directly on total bacterial extracts.
B- Schematic of the mitotic kinase cascade reconstituted in *E. coli.* The activated ERK kinase phosphorylates Bora at multiple sites including S112 (M3 motif), which binds and activates non-phosphorylated AURKA (AURKA^{T288V}) towards the Plk1 kinase domain.
C-D- Western blot analysis of total bacterial extracts reconstituting pBora$^{1-224}$ and AURKA^{T288V}-dependent T-loop (T210) phosphorylation of the Plk1 kinase domain (Plk1^{Kdom}) (**C**) or the isolated T-loop fused to GST (GST^{T-loop}) (**D**). Blots were probed with antibodies to Bora, phospho-T210 Plk1, or pan Plk1 (**C**) or GST (**D**), and AURKA (from top to bottom). ERK K-dead: kinase dead. Asterisk denotes a nonspecific band.
E- Schematic of MITOKINAC using Genetic Code Expansion to produce Bora$^{1-224,}$ uniquely phosphorylated at Serine 112, thus bypassing the need for a priming phosphorylation by ERK. The schematic illustrates the translation of Bora$^{1-224}$ (orange) by ribosomes (grey) in *E. coli,* which inserts a phospho-Serine (orange) at the amber

codon UAG. When produced and phosphorylated at S112, pBora$^{1-224}$ binds to and activates AURKA, which subsequently phosphorylates the Plk1 T-loop (T210).

F- Western blot analysis of total bacterial extracts reconstituting pBora and AURKA^{T288V}-dependent T-loop (T210) phosphorylation of the Plk1 kinase domain (Plk1^{Kdom}) using Genetic code expansion. Bacteria were transformed with a plasmid expressing wild-type Bora$^{1-224}$ (lanes 1-2) or Bora$^{1-224}$ harboring the amber codon TAG at position S112 (lanes 3-4). Blots were probed with antibodies to Bora, phospho-T210 Plk1, GST, and AURKA (from top to bottom). ERK K-dead: kinase dead.

Figure 5: **Bora$^{18-120}$ binds AURKA through hydrophobic anchors to position the essential phosphosite (pS112) in the AURKA active site.**

A- Multiple protein sequence alignments of the M1 motif of Bora. Identical residues are in dark blue. The mutated residues and the nature of the substitutions are indicated at the bottom of the alignment. The impact of the mutation on Bora's function is indicated by the rectangle's color around the amino acids. Green rectangles mean no effect, while red rectangles indicate a loss of function.

B- Western blot analysis of bacterial extracts reconstituting the mitotic kinase cascade in *E. coli* BL21, resulting in T-loop (T210) phosphorylation of the Plk1 kinase domain (Plk1^{Kdom}) using wild-type and Bora mutants of the M1 motif. Blots were probed with antibodies to Bora, phospho-T210 Plk1, or pan Plk1, and AURKA (from top to bottom). ERK K-dead: kinase dead.

C- View of the extended M1 motif of Bora bound to AURKA predicted by AlphaFold3. The M1 motif of Bora is anchored at one end by F25 binding to the F pocket of and V44, and F45 binding to the Y pocket of AURKA, respectively.

D- Western blot analysis of 2-step kinase reactions carried out with MBP-Bora$^{18-120}$ wild-type or mutant phosphorylated (+) or not (−) by the ERK kinase (step 1) in the presence of Plk1^{KDom} (substrate) and AURKA^{T288V} (step 2). Blots were probed with antibodies to Bora, phosphoT210 Plk1, or pan Plk1, and AURKA, as indicated (from top to bottom).

E- Multiple protein sequence alignments of the M2 and M3 motifs of Bora. Identical residues are shown in dark blue. The mutated residues and the nature of the substitutions are indicated at the bottom of the alignment. The impact of the mutation on Bora's function is indicated by the rectangle's color around the amino acids. Green rectangles indicate no effect, while red rectangles indicate a loss of function.

F- Western blot analysis of bacterial extracts reconstituting the mitotic kinase cascade in *E. coli* BL21, resulting in T-loop (T210) phosphorylation of the Plk1 kinase domain

(Plk1^{Kdom}) using wild-type and Bora mutants of the M2 and M3 motifs. Blots were probed with antibodies to Bora, phospho-T210 Plk1, or pan Plk1, and AURKA (from top to bottom). ERK K-dead: kinase dead. Note that Bora F103D and F104D mutants are expressed in *E. coli* (see panel H) but not detected by our anti-Bora antibody.

G- View of the M2 and M3 motifs of Bora bound to AURKA predicted by AF3. AURKA is shown as a surface colored according to electrostatic potential, with blue indicating positive and red indicating negative. Bora is shown as an orange ribbon. Bora residues F103 and F104 bind to the W pocket of AURKA, while pS112 engages an electropositive pocket.

H- Western blot analysis of 2-step kinase reactions carried out with MBP-Bora$^{18-120}$ wild-type or mutant phosphorylated (+) or not (−) by the ERK kinase (step 1) in the presence of Plk1^{KDom} (substrate) and AURKA^{T288V} (step 2). Blots were probed with antibodies to MBP, phosphoT210 Plk1, or pan Plk1, and AURKA, as indicated (from top to bottom). ERK K-dead: kinase dead. As membranes were sequentially revealed with different antibodies, the orange asterisk indicates the signal revealed by the anti-Bora antibody.

Figure 6: **pBora selectively activates AURKA towards the Plk1 T-loop via a novel evolutionarily conserved motif predicted to bind the Plk1 kinase domain.**

A- Multiple protein sequence alignments of the Bora region located between the M1 and M2/M3 motifs. Identical residues are shown in dark blue. The residues mutated, and the nature of the substitutions are indicated at the bottom of the alignment. The impact of the mutations on Bora's function is indicated by the rectangle's color around the amino acids. Green rectangles indicate no effect, while red rectangles indicate a loss of function.

B- Western blot analysis of bacterial extracts reconstituting the mitotic kinase cascade in *E. coli* BL21, resulting in T-loop (T210) phosphorylation of the Plk1 kinase domain (Plk1^{Kdom}) using wild-type and Bora mutants. Blots were probed with antibodies to Bora, phospho-T210 Plk1, or pan Plk1, and AURKA (from top to bottom). ERK K-dead: kinase dead.

C- Schematic of the two-step *in vitro* reconstitution of T-loop phosphorylation on T210 of the Plk1 kinase domain (pT210) by AURKA^{T288V} and pBora$^{18-120}$. In step 1, pBora$^{18-120}$ is incubated 1h at 30°C with the ERK kinase and Mg/ATP. In step 2, the reaction mix in step 1 is incubated in the presence of Mg/ATP with AURKA^{T288V} and Plk1^{KDom} for 30 minutes at 30°C.

D- Western blot analysis of 2-step kinase reactions carried out with MBP-Bora$^{18-120}$ wild-type or mutant phosphorylated (+) or not (−) by the ERK kinase (step 1) in the presence of Plk1^{KDom} (substrate) and AURKA^{T288V} (step 2). Blots were probed with antibodies to Bora, phosphoT210 Plk1, or pan Plk1, and AURKA, as indicated (from top to bottom). As membranes were sequentially revealed with different antibodies, the orange asterisk indicates the signal revealed by the anti-Bora antibody.

E- Schematic of the two-step *in vitro* reconstitution of T-loop phosphorylation on T210 of the isolated Plk1 T-loop fused to GST by AURKA^{T288V} and pBora$^{18-120}$. In step 1, pBora$^{18-120}$ is incubated 1h at 30°C with the ERK kinase and Mg/ATP. In step 2, the reaction mix in step 1 is incubated in the presence of Mg/ATP with AURKA^{T288V} and the isolated Plk1 T-loop fused to GST for 30 minutes at 30°C.

F- Western blot analysis of 2-step kinase reactions carried out with MBP-Bora$^{18-120}$ wild-type or mutant phosphorylated (+) or not (−) by the ERK kinase (step 1) in the presence of the T-loop of Plk1 (aa190-225) fused to GST (substrate) and AURKA^{T288V} (step 2). Blots were probed with antibodies to Bora, phosphoT210 Plk1, GST, and AURKA, as indicated (from top to bottom).

G- Schematic of the two-step *in vitro* reconstitution of Histone 3 phosphorylation on Serine 10 (pS10) by AURKA^{T288V} and pBora$^{18-120}$. In step 1, pBora$^{18-120}$ is incubated 1h at 30°C with the ERK kinase and Mg/ATP. In step 2, the reaction mix in step 1 is incubated in the presence of Mg/ATP with AURKA^{T288V} and Histone H3 for 30 minutes at 30°C.

H- Western blot analysis of 2-step kinase reactions carried out with MBP-Bora$^{18-120}$ wild-type or mutant phosphorylated (+) or not (−) by the ERK kinase (step 1) in the presence of Histone H3 (substrate) and AURKA^{T288V} (step 2). Blots were probed with antibodies to Bora, phosphoSer10 Histone H3, or pan Histone H3, and AURKA, as indicated (from top to bottom).

Figure 7: pBora engages the Alpha C helix of Plk1 to deliver AURKA activity to the Plk1 T-loop.

A- AlphaFold 3 model of the trimeric complex composed of pBora$^{18-120.}$ (orange), AURKA (grey), and the Plk1 kinase domain (blue). The residue T210 of the Plk1 T-loop, T288 of the AURKA T-loop, and the phosphorylated residue S112 of Bora are highlighted in red.

B- C- Zoom in view of the AURKA/Bora/Plk1 interface, highlighting contacting residues. Color scheme as in panel A.

D- Western blot analysis of 2-step kinase reactions carried out with MBP-Bora$^{18-120}$ wild-type or mutant phosphorylated (+) or not (−) by the ERK kinase (step 1) in the presence of the Plk1 kinase domain (substrate) and AURKA^{T288V} (step 2). Blots were probed with antibodies to Bora, phospho-T210 of Plk1, or pan Plk1, and AURKA, as indicated (from top to bottom).

E- The graph presents the normalized quantification of pT210 Plk1 signal over Plk1 from n=3 independent experiments.

Figure 8: Disrupting the Bora-Plk1 interface prevents mitotic entry in Xenopus egg extracts.

A- Schematic for the structure-function analysis of Bora during mitotic entry in Xenopus egg extracts. Interphase extracts (red) were depleted with Bora antibodies, and 30 min later supplemented with Bora$^{18-120}$ fragments (pre-phosphorylated by the ERK kinase) and with the recombinant human Gwl^{K72M} hyperactive kinase to force mitotic entry. Samples were collected at different time points and analyzed by Western blot (0, 20, 40 min) using mitotic markers to determine whether the extracts entered mitosis (green). The Western blot shows endogenous Bora levels before (Input) and after (Sn: supernatant) immunodepletion (Ip) from Xenopus egg extracts.

B- Interphase extracts were immunodepleted using anti-Bora antibodies and 30 min later supplemented with recombinant hyperactive human Gwl kinase (Gwl^{K72M}) and Bora$^{18-120}$ wild-type or variants pre-phosphorylated by ERK. A fraction of the extracts was collected at the indicated time-points (0, 20, 40 min) and analyzed by Western blot using specific antibodies to monitor the levels of Hu and Xe Gwl, Plk1, and Hu Bora as well as phosphorylation of Plx1 on T201 (pPlk1), and Cdk on Tyr15 (pTyr).

Supplementary Information

Molecular basis for the activation of Aurora A and Plk1 kinases by Bora during mitotic entry

Pillan A[1,2], Ormancey P[1,2], Ben Choug C[3], Orlicky S[4], Tavernier N[1,2], Van Hove L[1,2], Ossareh-Nazari B[1,2], Joly N[1,2], Sicheri F[4], Lorca T[3] and Pintard L[1,2]

[1] Université Paris cité, CNRS, Institut Jacques Monod, F-75013 Paris, France

[2] Programme Equipe Labellisée Ligue contre le Cancer

[3] Centre de Recherche de Biologie cellulaire de Montpellier, UMR 5237, Université de Montpellier, CNRS, 1919 Route de Mende, 34293 Montpellier Cedex 5, France

[4] Centre for Systems Biology, Lunenfeld Tanenbaum Research Institute, Sinai Health System, Toronto, ON M5G 1X5, Canada; Department of Molecular Genetics, University of Toronto, Toronto, ON M5S 1A8, Canada; Department of Biochemistry, University of Toronto, Toronto, ON M5S 1A8, Canada

Correspondance : lionel.pintard@ijm.fr

Supplementary Figures:

Supplementary Figure S1: AlphaFold 3 model of pBora bound to AURKA compared to the structure of Cep192 or TACC3 fragments bound to AURKA.

A- Superposition of the five pBora•AURKA complex predictions generated by Alphafold 3. AURKA is in grey and Bora is in orange. The predicted template modelling (pTM) score and the interface predicted template modelling (ipTM) scores are indicated.

B- Superposition of the predicted pBora•AURKA AlphaFold 3 model with the TACC3•AURKA structure [PDB: 5ODT https://doi.org/10.2210/pdb5ODT/pdb**]**) [67]. AURKA is shown as grey surface.

C- Superposition of the predicted pBora•AURKA AlphaFold 3 model with the Cep192•AURKA structure (PDB: 8PR7 [https://doi.org/10.2210/pdb8PR7/pdb**]**) [65]. AURKA is shown as grey surface.

D- Cartoon representation of the R-Spine assembly in the AURKA•pBora model predicted by Alphafold3. The R-Spine comprises L196, Q185, F274, and H254 residues (magenta). The « DFG » motif adopts the inward "in" position. When bound to pBora, AURKA exhibits the structural features of an active kinase.

Supplementary Figure S2: Mutation of the Bora-specific motif does not affect phosphorylation of the isolated Plk1 T-loop by AURKA^{T288V}

A- (i) View of the M1 and M2 motifs of Bora bound to AURKA predicted by AlphaFold 3**.** The Bora residues F25, V44, and F45 of the M1 motif binding to the F (green) and Y (yellow) pockets, as well as the residues F103 and F104 of the M2 motif binding to the W pocket (magenta), are shown. (ii) View of the Bora-specific motif bound to AURKA. I60 and I71 (blue arrows) anchor the motif to AURKA, whereas other hydrophobic and aromatic residues such as F56, W58, and I66 (red arrows) are solvent-exposed.
(iii) View of the Bora segment comprising amino acids 60 to 79 bound to AURKA.

B- Western blot analysis of total bacterial extracts reconstituting pBora and AURKA^{T288V}-dependent T-loop (T210) phosphorylation of the isolated Plk1 T-loop fused to GST (GST$^{T\text{-}loop}$). Blots were probed with antibodies to Bora, phospho-T210 Plk1, GST, and AURKA (from top to bottom). ERK K-dead: kinase dead.

Supplementary Figure S3: Details on the structural modeling of *H. sapiens* pBora•AURKA•Plk1^{KDom} complex generated by Alphafold 3

A- Structural alignment of the five pBora•AURKA•Plk1^{KDom} complex predictions generated by Alphafold 3 in a 1:1:1 binding stoichiometry. AURKA is in grey, Plk1 is in blue, and Bora is in orange. The predicted template modelling (pTM) score and the interface predicted template modelling (ipTM) scores are indicated.

B- Predicted Alignment Error (PAE) map calculated by AlphaFold3 showing the confidence of the distances between the residues in contact in the H. sapiens AURKA (126-403) (grey) • Bora (18-116) (orange) • Plk1 (1-332) (blue) complex generated by AlphaFold 3 in a 1:1:1 binding stoichiometry.

C- Per-residue confidence (pLDDT) of the pBora•AURKA•Plk1^{KDom} complex predicted by AlphaFold 3.

SUPPLEMENTARY TABLES:

Supplementary Table 1: Plasmids used in this study

Backbone	Insert	Cloning methods	ID/Source
pET	6xHis-ERK2-MEK1_R4F		Addgene#39212 [59]
pETM30-2	6xHis-GST-TEV-AURKA	CRE oNT37-38	pNT256 [59]
pETM30-2	6xHis-GST-TEV-AURKA^{T288V}	SDM pNT256 oNT123-124	pNT257 [59]
pDONR201	TEV-Bora$^{1-224}$	Gateway oLP989-990	pLP1848 [59]
pDEST17	6xHis-TEV-Bora$^{1-224}$	Gateway oLP989-990	pLP1850 [59]
pGEX-2T	GST-TEV-Plk1$^{1-330}$ [K82R]	CRE pNT179 oNT118-119	pLP2032 [59]
pCDFDuet1	GST-TEV-Plk1$^{1-330}$ [K82R]	CRE oLP2195-2196	pLP2228
pDNOR201	TEV-Bora$^{18-120}$	Gateway oLP1994-1997	pLP2072
pCDFDuet1	GST-Plk1 T-loop (aa 190-225)	CRE oLP2804-2805	pLP2546
pRSFDuet-1	Bora$^{1-224}$-TEV-6xHis / Strep-TEV-AURKA^{T288V}	CRE oLP1917-2116 oLP2132-2133	pLP2200
pRSFDuet-1	Strep-TEV-AURKA^{T288V}	CRE oLP2132-2133	pLP2204
pRSFDuet-1	Bora$^{1-224}$[S112A]-TEV-6xHis / Strep-TEV-AURKA^{T288V}	SDM pLP2200 oLP978-979	pLP2508
pET	6xHis-ERK2 [K52R]-MEK1_R4F	SDM pLP2401 oLP2806-2807	pLP2548
pKW2	SepRS(2)/pSertRNA(B4)/EF-Sep		Addgene #173897
pRSFDuet-1	Bora$^{1-224}$-TEV-(6xHis)- Strep-TEV-AURKA^{T288V} [TAA Stop]	CRE oLP1917-2116 oLP2132-3546	pLP3007
pET28b	Bora$^{1-224}$-TEV-6xHis [S112-TAG Amber codon]	SDM oLP1880-1881	pLP1988
pRSFDuet-1	Bora$^{1-224}$ [S112-TAG Amber codon]TEV (6xHis)-Strep-TEV-AURKA^{T288V} [TAA Stop]	CRE oLP1917-2116 oLP2132-3546	pLP2855
pRSFDuet-1	Bora$^{1-224}$ [F25D]-TEV-6xHis / Strep-TEV-AURKA^{T288V}	SDM pLP2200 oLP3488-3489	pLP2844
pRSFDuet-1	Bora$^{1-224}$ [E26R]-TEV-6xHis / Strep-TEV-AURKA^{T288V}	SDM pLP2200 oLP3490-3491	pLP2845
pRSFDuet-1	Bora$^{1-224}$ [E26A]-TEV-6xHis / Strep-TEV-AURKA^{T288V}	SDM pLP2200 oLP3492-3493	pLP2846
pRSFDuet-1	Bora$^{1-224}$ [D30R]-TEV-6xHis / Strep-TEV-AURKA^{T288V}	SDM pLP2200 oLP3494-3495	pLP2847
pRSFDuet-1	Bora$^{1-224}$ [Y31D]-TEV-6xHis / Strep-TEV-AURKA^{T288V}	SDM pLP2200 oLP3496-3497	pLP2848
pRSFDuet-1	Bora$^{1-224}$ [L39D]-TEV-6xHis / Strep- TEV-AURKA^{T288V}	SDM pLP2200 oLP3498-3499	pLP2849
pRSFDuet-1	Bora$^{1-224}$ [V44D]-TEV-6xHis / Strep- TEV-AURKA^{T288V}	SDM pLP2200 oLP3500-3501	pLP2850
pRSFDuet-1	Bora$^{1-224}$ [F45D]-TEV-6xHis / Strep- TEV-AURKA^{T288V}	SDM pLP2200 oLP2771-2772	pLP2530

pRSFDuet-1	Bora$^{1-224}$ [V44D-F45D]-TEV-6xHis / Strep- TEV-AURKA^{T288V}	SDM pLP2200 oLP3502-3503	pLP2851
pRSFDuet-1	Bora$^{1-224}$ [K46E]-TEV-6xHis / Strep- TEV-AURKA^{T288V}	SDM pLP2200 oLP3504-3505	pLP2852
pRSFDuet-1	Bora$^{1-224}$ [T48V]-TEV-6xHis / Strep- TEV-AURKA^{T288V}	SDM pLP2200 oLP3506-3507	pLP2853
pRSFDuet-1	Bora$^{1-224}$ [L34D]-TEV-6xHis / Strep- TEV-AURKA^{T288V}	SDM pLP2200 oLP2769-2770	pLP2529
pRSFDuet-1	Bora$^{1-224}$ [R57D]-TEV-6xHis / Strep- TEV-AURKA^{T288V}	SDM pLP2200 oLP3508-3509	pLP2859
pRSFDuet-1	Bora$^{1-224}$ [S59E]-TEV-6xHis / Strep- TEV-AURKA^{T288V}	SDM pLP2200 oLP3512-3513	pLP2860
pRSFDuet-1	Bora$^{1-224}$ [S59R]-TEV-6xHis / Strep- TEV-AURKA^{T288V}	SDM pLP2200 oLP3510-3511	pLP2861
pRSFDuet-1	Bora$^{1-224}$ [D61A]-TEV-6xHis / Strep- TEV-AURKA^{T288V}	SDM pLP2200 oLP3514-3515	pLP2862
pRSFDuet-1	Bora$^{1-224}$ [V69D]-TEV-6xHis / Strep- TEV-AURKA^{T288V}	SDM pLP2200 oLP3516-3517	pLP2863
pRSFDuet-1	Bora$^{1-224}$ [E70R]-TEV-6xHis / Strep- TEV-AURKA^{T288V}	SDM pLP2200 oLP3518-3519	pLP2864
pRSFDuet-1	Bora$^{1-224}$ [I71D]-TEV-6xHis / Strep- TEV-AURKA^{T288V}	SDM pLP2200 oLP3520-3521	pLP2865
pRSFDuet-1	Bora$^{1-224}$ [D72R]-TEV-6xHis / Strep- TEV-AURKA^{T288V}	SDM pLP2200 oLP3522-3523	pLP2866
pRSFDuet-1	Bora$^{1-224}$ [I76D]-TEV-6xHis / Strep- TEV-AURKA^{T288V}	SDM pLP2200 oLP3526-3527	pLP2867
pRSFDuet-1	Bora$^{1-224}$ [Q79R]-TEV-6xHis / Strep- TEV-AURKA^{T288V}	SDM pLP2200 oLP3528-3529	pLP2868
pRSFDuet-1	Bora$^{1-224}$ [F56D]-TEV-6xHis / Strep- TEV-AURKA^{T288V}	SDM pLP2200 oLP3605-3606	pLP2895
pRSFDuet-1	Bora$^{1-224}$ [W58D]-TEV-6xHis / Strep- TEV-AURKA^{T288V}	SDM pLP2200 oLP3607-3608	pLP2896
pRSFDuet-1	Bora$^{1-224}$ [I60D]-TEV-6xHis / Strep- TEV-AURKA^{T288V}	SDM pLP2200 oLP2775-2776	pLP2532
pRSFDuet-1	Bora$^{1-224}$ [Q62R]-TEV-6xHis / Strep- TEV-AURKA^{T288V}	SDM pLP2200 oLP3629-3630	pLP2908
pRSFDuet-1	Bora$^{1-224}$ [I66D]-TEV-6xHis / Strep- TEV-AURKA^{T288V}	SDM pLP2200 oLP3609-3610	pLP2897
pRSFDuet-1	Bora$^{1-224}$ [P68D]-TEV-6xHis / Strep- TEV-AURKA^{T288V}	SDM pLP2200 oLP2779-2780	pLP2534
pRSFDuet-1	Bora$^{1-224}$ [D91R]-TEV-6xHis / Strep- TEV-AURKA^{T288V}	SDM pLP2200 oLP2783-2784	pLP2536
pRSFDuet-1	Bora$^{1-224}$ [E93R]-TEV-6xHis / Strep- TEV-AURKA^{T288V}	SDM pLP2200 oLP2785-2786	pLP2537
pRSFDuet-1	Bora$^{1-224}$ [Q97A]-TEV-6xHis / Strep- TEV-AURKA^{T288V}	SDM pLP2200 oLP2787-2788	pLP2538
pRSFDuet-1	Bora$^{1-224}$ [E101R]-TEV-6xHis / Strep- TEV-AURKA^{T288V}	SDM pLP2200 oLP3530-3531	pLP2869
pRSFDuet-1	Bora$^{1-224}$ [F103D]-TEV-6xHis / Strep- TEV-AURKA^{T288V}	SDM pLP2200 oLP3532-3533	pLP2870
pRSFDuet-1	Bora$^{1-224}$ [F104D]-TEV-6xHis / Strep- TEV-AURKA^{T288V}	SDM pLP2200 oLP3534-3535	pLP2871
pRSFDuet-1	Bora$^{1-224}$ [I109R]-TEV-6xHis / Strep- TEV-AURKA^{T288V}	SDM pLP2200 oLP3538-3539	pLP2873
pRSFDuet-1	Bora$^{1-224}$ [I109D]-TEV-6xHis / Strep- TEV-AURKA^{T288V}	SDM pLP2200 oLP3540-3541	pLP2874
pRSFDuet-1	Bora$^{1-224}$ [V110R]-TEV-6xHis / Strep- TEV-AURKA^{T288V}	SDM pLP2200 oLP3542-3543	pLP2875
pRSFDuet-1	Bora$^{1-224}$ [P111D]-TEV-6xHis / Strep- TEV-AURKA^{T288V}	SDM pLP2200 2789-2790	pLP2539

pMAL-C2	MBP-TEV-Bora$^{18-120}$	Gateway oLP1994-1997	pLP2784
pMAL-C2	MBP-TEV-Bora$^{18-120}$ [F25D]	SDM pLP2784 oLP3488-3489	pLP2915
pMAL-C2	MBP-TEV-Bora$^{18-120}$ [V44D-F45D]	SDM pLP2784 oLP3502-3503	pLP2987
pMAL-C2	MBP-TEV-Bora$^{18-120}$ [S112A]	SDM pLP2784 oLP978-979	pLP2928
pMAL-C2	MBP-TEV-Bora$^{18-120}$ [F103D]	SDM pLP2784 oLP3532-3533	pLP2988
pMAL-C2	MBP-TEV-Bora$^{18-120}$ [F104D]	SDM pLP2784 oLP3534-3535	pLP2995
pMAL-C2	MBP-TEV-Bora$^{18-120}$ [F56D]	SDM pLP2784 oLP3605-3606	pLP2916
pMAL-C2	MBP-TEV-Bora$^{18-120}$ [W58D]	SDM pLP2784 oLP3607-3608	pLP2917
pMAL-C2	MBP-TEV-Bora$^{18-120}$ [S59R]	SDM pLP2784 oLP3510-3511	pLP2918
pMAL-C2	MBP-TEV-Bora$^{18-120}$ [I60D]	SDM pLP2784 oLP2775-2776	pLP2919
pMAL-C2	MBP-TEV-Bora$^{18-120}$ [Q62R]	SDM pLP2784 oLP3629-3630	pLP2920
pMAL-C2	MBP-TEV-Bora$^{18-120}$ [I66D]	SDM pLP2784 oLP3609-3610	pLP2921
pCDFDuet1	GST-TEV-Plk1$^{1-330}$ [K82R, R48D]	SDM pLP2228 oLP3651-3652	pLP2974
pCDFDuet1	GST-TEV-Plk1$^{1-330}$ [K82R, R95A]	SDM pLP2228 oLP3615-3616	pLP2902
pCDFDuet1	GST-TEV-Plk1$^{1-330}$ [K82R, R106A]	SDM pLP2228 oLP3644-3645	pLP2955
pCDFDuet1	GST-TEV-Plk1$^{1-330}$ [K82R, E121A]	SDM pLP2228 oLP3621-3622	pLP2905

*SDM: Site-directed Mutagenesis, °CRE: Cloning by restriction enzymes

Supplementary Table 2: **List of primers used in this study**

Purpose and sequences	ID
Forward and reverse primers to amplify and clone AURKA in pETM30 NcoI/XhoI (pNT256): CGCCATGGACCGATCTAAAGAAAAC-F GGCCTCGAGCTAAGACTGTTTGCTAGCTG-R	oNT37 oNT38
Forward and reverse primers for AURKA^{T288V} (pNT257): GCTCCATCCTCCAGGAGGACCGTCCTCTGTGGCACCCTGGACTACC-F GGTAGTCCAGGGTGCCACAGAGGACGGTCCTCCTGGAGGATGGAGC-R	oNT123 oNT124
Forward and reverse primers to clone Bora$^{1-224}$ Gateway (pLP1848-pLP1850): GGGGACAAGTTTGTACAAAAAAGCAGGCTTCATGGGAGATGTCAAGGAATCAAAG-F GGGGACCACTTTGTACAAGAAAGCTGGGTCCTACTCTAGTGATGTTTGAACACC-R	oLP989 oLP990
Forward and reverse primers for Plk1$^{1-330}$ mutagenesis K82R (pLP2032): GAGGTGTTCGCGGGCCGGATTGTGCCTAAGTCTCTGCT-F AGCAGAGACTTAGGCACAATCCGGCCCGCGAACACCTC-R	oNT118 oNT119
Forward and reverse primers for GST-TEV-Plk1$^{1-330}$ K82R insertion into pCDFDuet-1 (pLP2228) TATACAATTGGATGTCCCCTATACTAGGTTATTGG-F CAGAGGTACCTTAGCTGGGAGCAATCGAAAAC-R	oLP2195 oLP2196
Forward and reverse primers to clone TEV-Bora$^{18-120}$ (pLP2072) Gateway GGGGACAAGTTTGTACAAAAAAGCAGGCTTCCCAACGACCGAAAACCTGTATTTTCAGGGCGCCATGGATCCGGAATTCAGGATCCCTGTTTTAAATCCTTTTG-F GGGGACCACTTTGTACAAGAAAGCTGGGTCTTATTTCCCTTCATGATCAGTCCAAG-R	oLP1994 oLP1997
Forward and reverse primers for GST-Plk1 T-loop 190-225 (pLP2546) ATGGATCCGGAATTCAAAATAGGGGATTTTGGAC-F CTCGAGGGTACCTTACTTGCTCAGCACCTCGGGAG-R	oLP2804 oLP2805
Forward and reverse primers to amplify and clone Bora$^{1-224}$-TEV-6xHis in pRSF-Duet (pLP2200) GGGCCATGGGAGATGTCAAGGAATCAAAG-F CCGGAATTCGGTCAGTGGTGGTGGTGGTGGTGGAATCCTTGGAAGTATAGATTTTCACCCTCTAGTGATGTTTGAACACCAC-R	oLP1917 oLP2116
Forward and reverse primers to amplify and clone Strep-TEV-AURKA^{T288V} in pRSF-Duet pLP2200) TATACATATGGCTAGCTGGAGCCACCCGCAGTTCGAAAAAGGATCTGGTGGTGGTGGTGGTGAAAACCTGTACTTCCAGGGAATGGACCGATCTAAAGAAAACTGC-F CAGACTCGAGCTAAGACTGTTTGCTAGCTG-R	oLP2132 oLP2133
Forward and reverse primers to amplify and clone Strep-TEV-AURKA^{T288V} in pLP2204 TATACATATGGCTAGCTGGAGCCACCCGCAGTTCGAAAAAGGATCTGGTGGTGGTGGTGGTGAAAACCTGTACTTCCAGGGAATGGACCGATCTAAAGAAAACTGC-F CAGACTCGAGCTAAGACTGTTTGCTAGCTG-R	oLP2132 oLP2133
Forward and reverse primers for SDM Bora$^{1-224}$[S112A]-TEV-6xHis in pLP2200. GATGTCATCGTACCCGCTCCTTGGACTGATCATGAAGG-F CCTTCATGATCAGTCCAAGGAGCGGGTACGATGACATC-R	oLP978 oLP979
Forward and reverse primers for SDM pLP2401 6xHis-ERK2 [K52R]-MEK1_R4F (pLP2548). CAAAGTTCGAGTTGCTATCCGGAAAATCAGTCCTTTTGAGC-F GCTCAAAAGGACTGATTTTCCGGATAGCAACTCGAACTTTG-R	oLP2806 oLP2807

Forward and reverse primers for SDM Bora$^{1-224}$ [S112-TAG Amber codon] in pET28b (pLP1988). CACTAAAGATGTCATCGTACCCTAGCCTTGGACTGATCATGAAGGG-F CCCTTCATGATCAGTCCAAGGCTAGGGTACGATGACATCTTTAGTG-R	oLP1880 oLP1881
Forward and reverse primers to amplify and clone Bora$^{1-224}$ with TEV-(6xHis) in pRSF-Duet pLP3007. GGGCCATGGGAGATGTCAAGGAATCAAAG-F CCGGAATTCGGTCAGTGGTGGTGGTGGTGGTGGAATCCTTGGAAGTATAGATT TTCACCCTCTAGTGATGTTTGAACACCAC-R	oLP1917 oLP2116
Forward and reverse primers to amplify, clone and mutate the stop codon of Strep-TEV-AURKA^{T288V} [TAA Stop] in pRSF-Duet pLP3007 TATACATATGGCTAGCTGGAGCCACCCGCAGTTCGAAAAAGGATCTGGTGGTG GTGGTGGTGAAAACCTGTACTTCCAGGGAATGGACCGATCTAAAGAAAACTGC-F CCAGACTCGAGTTAAGACTGTTTGCTAGCTGATTC-R	oLP2132 oLP3546
Forward and reverse primers for Bora$^{1-224}$ [S112-TAG Amber codon] TEV (6xHis) in pRSF-Duet pLP2855 GGGCCATGGGAGATGTCAAGGAATCAAAG-F CCGGAATTCGGTCAGTGGTGGTGGTGGTGGTGGAATCCTTGGAAGTATAGATT TTCACCCTCTAGTGATGTTTGAACACCAC-R	oLP1917 oLP2116
Forward and reverse primers for amplify, clone and mutated the stop codon of Strep-TEV-AURKA^{T288V} [TAA Stop] in pRSF-duet pLP2855 TATACATATGGCTAGCTGGAGCCACCCGCAGTTCGAAAAAGGATCTGGTGGTG GTGGTGGTGAAAACCTGTACTTCCAGGGAATGGACCGATCTAAAGAAAACTGC-F CCAGACTCGAGTTAAGACTGTTTGCTAGCTGATTC-R	oLP2132 oLP3546
Forward and reverse primers for Bora$^{1-224}$ [F25D]-TEV-6xHis in pLP2200 (pLP2844) CCCTGTTTTAAATCCTGATGAAAGTCCTAGTGAT-F CACTAGGACTTTCATCAGGATTTAAAACAGGGAT-R	oLP3488 oLP3489
Forward and reverse primers for Bora$^{1-224}$ [E26R]-TEV-6xHis in pLP2200 (pLP2845) CCCTGTTTTAAATCCTTTTCGTAGTCCTAGTGATTATTCT-F GAATAATCACTAGGACTACGAAAAGGATTTAAAACAGGGA-R	oLP3490 oLP3491
Forward and reverse primers for Bora$^{1-224}$ [E26A]-TEV-6xHis in pLP2200 (pLP2846) CCCTGTTTTAAATCCTTTTGCGAGTCCTAGTGATTATTCTA-F GAATAATCACTAGGACTCGCAAAAGGATTTAAAACAGGGA-R	oLP3492 oLP3493
Forward and reverse primers for Bora$^{1-224}$ [D30R]-TEV-6xHis in pLP2200 (pLP2847) CCTTTTGAAAGTCCTAGTCGTTATTCTAATCTCCATGA-F CATGGAGATTAGAATAACGACTAGGACTTTCAAAAGGAT-R	oLP3494 oLP3495
Forward and reverse primers for Bora$^{1-224}$ [Y31D]-TEV-6xHis in pLP2200 (pLP2848) GAAAGTCCTAGTGATGATTCTAATCTCCATGAACAA-F GAGTTTGTTCATGGAGATTAGAATCATCACTAGGACTTTCA-R	oLP3496 oLP3497
Forward and reverse primers for Bora$^{1-224}$ [L39D]-TEV-6xHis in pLP2200 (pLP2849) GAGTTTGTTCATGGAGATTAGAATCATCACTAGGACTTTCA-F GATTTAAAAACAGAAGGACTGGCGTCAGTTTGTTCATGGAGATT-R	oLP3498 oLP3499
Forward and reverse primers for Bora$^{1-224}$ [V44D]-TEV-6xHis in pLP2200 (pLP2850) CTCTCGCCAGTCCTTCTGATTTTAAATCAACAAAATTACCA-F GGTAATTTTGTTGATTTAAAATCAGAAGGACTGGCGAGAGT-R	oLP3500 oLP3501
Forward and reverse primers for Bora$^{1-224}$ [F45D]-TEV-6xHis in pLP2200 (pLP2530) GAACAAACTCTCGCCAGTCCTTCTGTTGATAAATCAACAAAATTACCAACTCCAG G-F CCTGGAGTTGGTAATTTTGTTGATTTATCAACAGAAGGACTGGCGAGAGTTTGTT C-R	oLP2771 oLP2772
Forward and reverse primers for Bora$^{1-224}$ [V44D-F45D]-TEV-6xHis in pLP2200 (pLP2851) CAAACTCTCGCCAGTCCTTCTGATGATAAATCAACAAAATTACCAACTCCA-F GGAGTTGGTAATTTTGTTGATTTATCATCAGAAGGACTGGCGAGAGTTTGT-R	oLP3502 oLP3503

Forward and reverse primers for Bora$^{1-224}$ [K46E]-TEV-6xHis in pLP2200 (pLP2852) CCAGTCCTTCTGTTTTTGAATCAACAAAATTACCA-F GGTAATTTTGTTGATTCAAAAACAGAAGGACTGGCGA-R	oLP3504 oLP3505
Forward and reverse primers for Bora$^{1-224}$ [T48V]-TEV-6xHis in pLP2200 (pLP2853) CCTTCTGTTTTTAAATCAGTGAAATTACCAACTCCA-F CCCTGGAGTTGGTAATTTCACTGATTTAAAAACAGA-R	oLP3506 oLP3507
Forward and reverse primers for Bora$^{1-224}$ [L34D]-TEV-6xHis in pLP2200 (pLP2529) GTGATTATTCTAATGACCATGAACAAACTCTCGCC-F GGCGAGAGTTTGTTCATGGTCATTAGAATAATCAC-R	oLP2769 oLP2770
Forward and reverse primers for Bora$^{1-224}$ [R57D]-TEV-6xHis in pLP2200 (pLP2859) CCAACTCCAGGGAAATTTGATTGGTCTATTGATCA-F GTTGATCAATAGACCAATCAAATTTCCCTGGAGT-R	oLP3508 oLP3509
Forward and reverse primers for Bora$^{1-224}$ [S59E]-TEV-6xHis in pLP2200 (pLP2860) GGGAAATTTAGATGGGAAATTGATCAACTAGCT-F CAGCTAGTTGATCAATTTCCCATCTAAATTTCCCT-R	oLP3512 oLP3513
Forward and reverse primers for Bora$^{1-224}$ [S59R]-TEV-6xHis in pLP2200 (pLP2861) GGGAAATTTAGATGGCGTATTGATCAACTAGCT-F CAGCTAGTTGATCAATACGCCATCTAAATTTCCCT-R	oLP3510 oLP3511
Forward and reverse primers for Bora$^{1-224}$ [D61A]-TEV-6xHis in pLP2200 (pLP2862) GGGAAATTTAGATGGTCTATTGCGCAACTAGCTGTAATAAATCCT-F GGATTTATTACAGCTAGTTGCGCAATAGACCATCTAAATTTCCCT-R	oLP3514 oLP3515
Forward and reverse primers for Bora$^{1-224}$ [V69D]-TEV-6xHis in pLP2200 (pLP2863) GCTGTAATAAATCCTGATGAAATAGACCCAGAAGA-F CTTCTGGGTCTATTTCATCAGGATTTATTACAGCT-R	oLP3516 oLP3517
Forward and reverse primers for Bora$^{1-224}$ [E70R]-TEV-6xHis in pLP2200 (pLP2864) GCTGTAATAAATCCTGTACGTATAGACCCAGAAGA -F CTTCTGGGTCTATACGTACAGGATTTATTACA-R	oLP3518 oLP3519
Forward and reverse primers for Bora$^{1-224}$ [I71D]-TEV-6xHis in pLP2200 (pLP2865) GCTGTAATAAATCCTGTAGAAGATGACCCAGAAGATATTCA-F CGATGAATATCTTCTGGGTCATCTTCTACAGGATTTATTACA-R	oLP3520 oLP3521
Forward and reverse primers for Bora$^{1-224}$ [D72R]-TEV-6xHis in pLP2200 (pLP2866) CCTGTAGAAATACGTCCAGAAGATATTCA-F CGATGAATATCTTCTGGACGTATTTCTACAGGA-R	oLP3522 oLP3523
Forward and reverse primers for Bora$^{1-224}$ [I76D]-TEV-6xHis in pLP2200 (pLP2867) GAAATAGACCCAGAAGATGATCATCGTCAAGCTTTATACT-F GTATAAAGCTTGACGATGATCATCTTCTGGGTCTATTTCT-R	oLP3526 oLP3527
Forward and reverse primers for Bora$^{1-224}$ [Q79R]-TEV-6xHis in pLP2200 (pLP2868) CCCAGAAGATATTCATCGTCGTGCTTTATACTTAAGTCA-F GACTTAAGTATAAAGCACGACGATGAATATCTTCTGGGT-R	oLP3528 oLP3529
Forward and reverse primers for Bora$^{1-224}$ [F56D]-TEV-6xHis in pLP2200 (pLP2895) CCAACTCCAGGGAAAGATAGATGGTCTATTGATC-F GATCAATAGACCATCTATCTTTCCCTGGAGTTGG-R	oLP3605 oLP3606
Forward and reverse primers for Bora$^{1-224}$ [W58D]-TEV-6xHis in pLP2200 (pLP2896) CTCCAGGGAAATTTAGAGACTCTATTGATCAACTA-F TAGTTGATCAATAGAGTCTCTAAATTTCCCTGGAG-R	oLP3607 oLP3608
Forward and reverse primers for Bora$^{1-224}$ [I60D]-TEV-6xHis in pLP2200 (pLP2532) GGGAAATTTAGATGGTCTGATGATCAACTAGCTGTAATAAATCC-F GGATTTATTACAGCTAGTTGATCATCAGACCATCTAAATTTCCC-R	oLP2775 oLP2776
Forward and reverse primers for Bora$^{1-224}$ [Q62R]-TEV-6xHis in pLP2200 (pLP2908) GATGGTCTATTGATCGCCTAGCTGTAATAAATCCT-F AGGATTTATTACAGCTAGGCGATCAATAGACCATC-R	oLP3629 oLP3630
Forward and reverse primers for Bora$^{1-224}$ [I66D]-TEV-6xHis in pLP2200 (pLP2897) GAAATTTAGATGGTCTGATGATCAACTAGCTGTAA-F TTACAGCTAGTTGATCATCAGACCATCTAAATTTC-R	oLP3609 oLP3610

Forward and reverse primers for Bora$^{1-224}$ [P68D]-TEV-6xHis in pLP2200 (pLP2534) CAACTAGCTGTAATAAATGATGTAGAAATAGACCCAGAAG-F CTTCTGGGTCTATTTCTACATCATTTATTACAGCTAGTTG-R	oLP2779 oLP2780
Forward and reverse primers for Bora$^{1-224}$ [D91R]-TEV-6xHis in pLP2200 (pLP2536) TTCTCGAATAGATAAACGTGTGGAAGACAAAAGAC-F GTCTTTTGTCTTCCACACGTTTATCTATTCGAGAA-R	oLP2783 oLP2784
Forward and reverse primers for Bora$^{1-224}$ [E93R]-TEV-6xHis in pLP2200 (pLP2537) CGAATAGATAAAGATGTGCGAGACAAAAGACAAAAAGC-F GCTTTTTGTCTTTTGTCTCGCACATCTTTATCTATTCG-R	oLP2785 oLP2786
Forward and reverse primers for Bora$^{1-224}$ [Q97A]-TEV-6xHis in pLP2200 (pLP2538) GTGGAAGACAAAAGAGCAAAAGCCATTGAAGAGTTTTTC-F GAAAAACTCTTCAATGGCTTTTGCTCTTTTGTCTTCCAC-R	oLP2787 oLP2788
Forward and reverse primers for Bora$^{1-224}$ [E101R]-TEV-6xHis in pLP2200 (pLP2869) GACAAAAGACAAAAAGCCATTCGTGAGTTTTTCACTAAAGATGTC-F GACATCTTTAGTGAAAAACTCACGAATGGCTTTTTGTCTTTTGTC-R	oLP3588 oLP3589
Forward and reverse primers for Bora$^{1-224}$ [F103D]-TEV-6xHis in pLP2200 (pLP2870) GACAAAAAGCCATTGAAGAGGATTTCACTAAAGATGTCATCGT-F CGATGACATCTTTAGTGAAATCCTCTTCAATGGCTTTTTGT-R	oLP3532 oLP3533
Forward and reverse primers for Bora$^{1-224}$ [F104D]-TEV-6xHis in pLP2200 (pLP2871) GCCATTGAAGAGTTTGACACTAAAGATGTCATCGT-F GGTACGATGACATCTTTAGTGTCAAACTCTTCAATGGCT-R	oLP3534 oLP3535
Forward and reverse primers for Bora$^{1-224}$ [I109R]-TEV-6xHis in pLP2200 (pLP2873) GAGTTTTTCACTAAAGATGTCCGCGTACCCTCTCCTTGGACT-F CAGTCCAAGGAGAGGGTACGCGGACATCTTTAGTGAAAAACT-R	oLP3538 oLP3539
Forward and reverse primers for Bora$^{1-224}$ [I109D]-TEV-6xHis in pLP2200 (pLP2874) GAGTTTTTCACTAAAGATGTCGACGTACCCTCTCCTTGGACT-F CAGTCCAAGGAGAGGGTACGTCGACATCTTTAGTGAAAAACT-R	oLP3540 oLP3541
Forward and reverse primers for Bora$^{1-224}$ [V110R]-TEV-6xHis in pLP2200 (pLP2875) CACTAAAGATGTCATCCGTCCCTCTCCTTGGACTGA-F CAGTCCAAGGAGAGGGACGGATGACATCTTTAGTGA-R	oLP3542 oLP3543
Forward and reverse primers for Bora$^{1-224}$ [P111D]-TEV-6xHis in pLP2200 (pLP2539) GAGTTTTTCACTAAAGATGTCATCGTAGACTCTCCTTGGACTGATCATGAAGG-F CCTTCATGATCAGTCCAAGGAGAGTCTACGATGACATCTTTAGTGAAAAACTC-R	oLP2789 oLP2790
Forward and reverse primers to clone MBP-TEV-Bora$^{18-120}$ WT by Gateway with pLP2072 (pLP2784) GGGGACAAGTTTGTACAAAAAAGCAGGCTTCCCAACGACCGAAAACCTGTATTT TCAGGGCGCCATGGATCCGGAATTCAGGATCCCTGTTTTAAATCCTTTTG-F GGGGACCACTTTGTACAAGAAAGCTGGGTCTTATTTCCCTTCATGATCAGTCCA AG-R	oLP1994 oLP1997
Forward and reverse primers for MBP-TEV-Bora$^{18-120}$ F25D (pLP2915) CCCTGTTTTAAATCCTGATGAAAGTCCTAGTGAT-F CACTAGGACTTTCATCAGGATTTAAAACAGGGAT-R	oLP3488 oLP3489
Forward and reverse primers for MBP-TEV-Bora$^{18-120}$ V44D-F45D (pLP2987) CAAACTCTCGCCAGTCCTTCTGATGATAAATCAACAAAATTACCAACTCCA -F GGAGTTGGTAATTTTGTTGATTTATCATCAGAAGGACTGGCGAGAGTTTGT-R	oLP3502 oLP3503
Forward and reverse primers for MBP-TEV-Bora$^{18-120}$ S112A (pLP2928) GATGTCATCGTACCCGCTCCTTGGACTGATCATGAAGG-F CCTTCATGATCAGTCCAAGGAGCGGGTACGATGACATC-R	oLP978 oLP979
Forward and reverse primers for MBP-TEV-Bora$^{18-120}$ F103D (pLP2988) GACAAAAAGCCATTGAAGAGGATTTCACTAAAGATGTCATCGT-F CGATGACATCTTTAGTGAAATCCTCTTCAATGGCTTTTTGT-R	oLP3532 oLP3533
Forward and reverse primers for MBP-TEV-Bora$^{18-120}$ F104D (pLP2995) GCCATTGAAGAGTTTGACACTAAAGATGTCATCGT-F GGTACGATGACATCTTTAGTGTCAAACTCTTCAATGGCT-R	oLP3534 oLP3535

Forward and reverse primers for MBP-TEV-Bora$^{18-120}$ F56D (pLP2916) CCAACTCCAGGGAAAGATAGATGGTCTATTGATC-F GATCAATAGACCATCTATCTTTCCCTGGAGTTGG-R	oLP3605 oLP3606
Forward and reverse primers for MBP-TEV-Bora$^{18-120}$ W58D (pLP2917) CTCCAGGGAAATTTAGAGACTCTATTGATCAACTA-F TAGTTGATCAATAGAGTCTCTAAATTTCCCTGGAG-R	oLP3607 oLP3608
Forward and reverse primers for MBP-TEV-Bora$^{18-120}$ S59R (pLP2918) GGGAAATTTAGATGGCGTATTGATCAACTAGCT-F CAGCTAGTTGATCAATACGCCATCTAAATTTCCCT-R	oLP3510 oLP3511
Forward and reverse primers for MBP-TEV-Bora$^{18-120}$ I60D (pLP2919) GGGAAATTTAGATGGTCTGATGATCAACTAGCTGTAATAAATCC-F GGATTTATTACAGCTAGTTGATCATCAGACCATCTAAATTTCCC-R	oLP2775 oLP2776
Forward and reverse primers for MBP-TEV-Bora$^{18-120}$ Q62R (pLP2920) GATGGTCTATTGATCGCCTAGCTGTAATAAATCCT-F AGGATTTATTACAGCTAGGCGATCAATAGACCATC-R	oLP3629 oLP3630
Forward and reverse primers for MBP-TEV-Bora$^{18-120}$ I66D (pLP2921) GAAATTTAGATGGTCTGATGATCAACTAGCTGTAA-F TTACAGCTAGTTGATCATCAGACCATCTAAATTTC-R	oLP3609 oLP3610
Forward and reverse primers for GST-TEV-Plk1$^{1-330}$ K82R-R48D (pLP2974) GGTCCTAGTGGACCCAGACAGCCGGCGGCGCTATG-F CATAGCGCCGCCGGCTGTCTGGGTCCACTAGGACC-R	oLP3651 oLP3652
Forward and reverse primers for GST-TEV-Plk1$^{1-330}$ K82R-R95A (pLP2902) GCTCAAGCCGCACCAGGCGGAGAAGATGTCCATGG-F CCATGGACATCTTCTCCGCCTGGTGCGGCTTGAGC-R	oLP3615 oLP3616
Forward and reverse primers for GST-TEV-Plk1$^{1-330}$ K82R-R106A (pLP2955) GGAAATATCCATTCACGCGAGCCTCGCCCACCAGC-F GCTGGTGGGCGAGGCTCGCGTGAATGGATATTTCC-R	oLP3644 oLP3645
Forward and reverse primers for GST-TEV-Plk1$^{1-330}$ K82R-E121A (pLP2905) GGATTCCACGGCTTTTTCGCGGACAACGACTTCGT-F ACGAAGTCGTTGTCCGCGAAAAAGCCGTGGAATCC-R	oLP3621 oLP3622

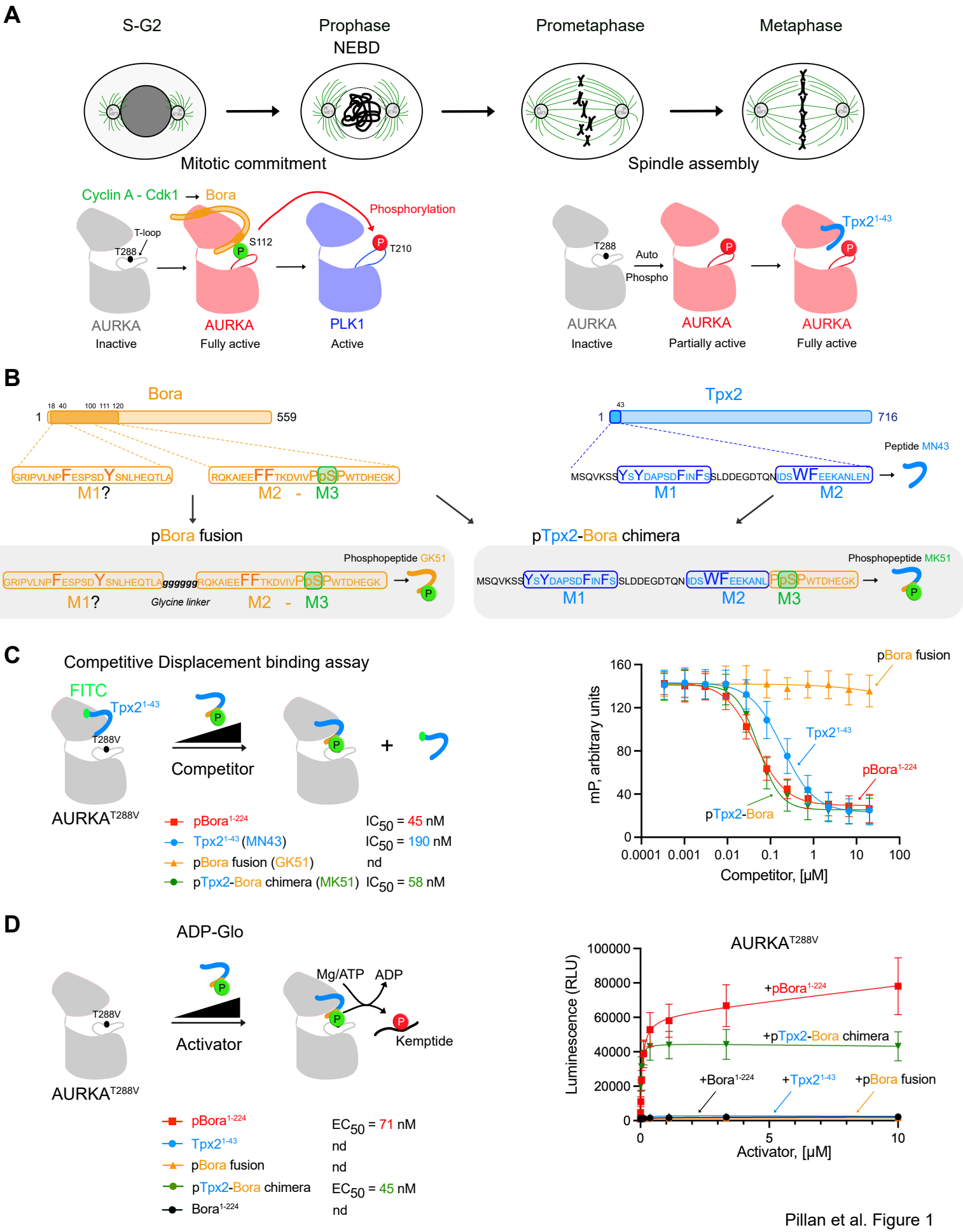

Pillan et al. Figure 1

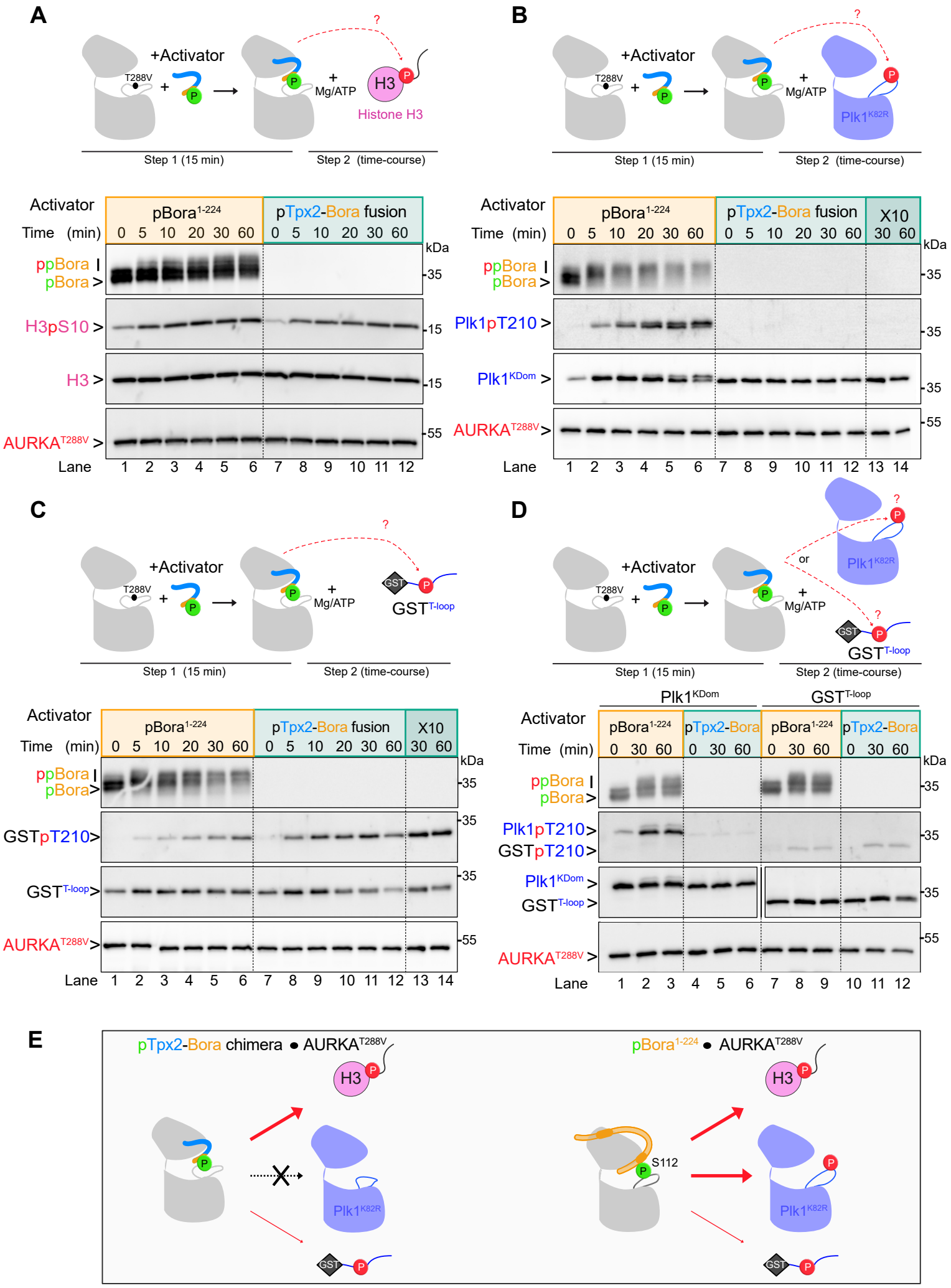

Pillan et al. Figure 2

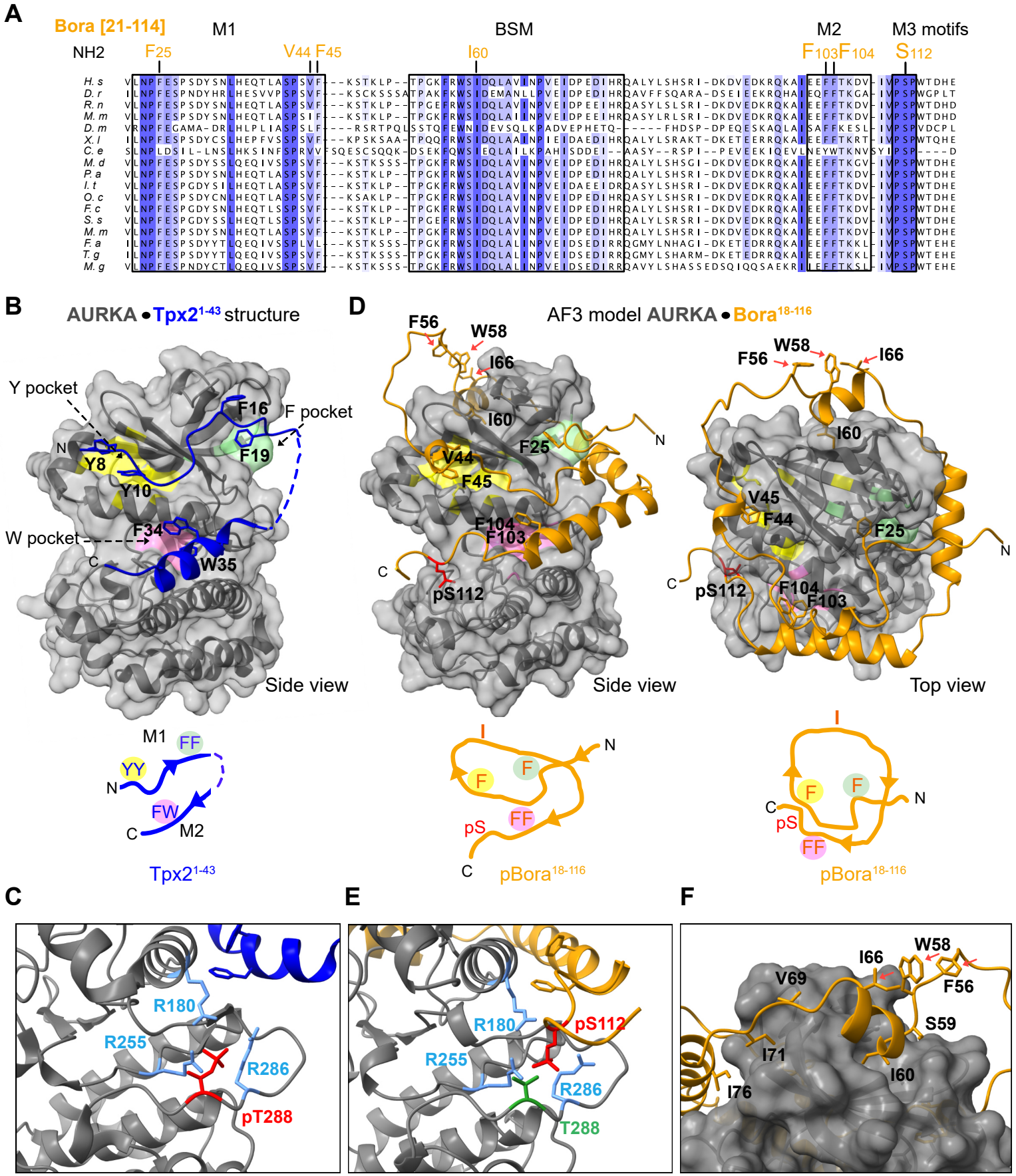

Pillan et al. Figure 3

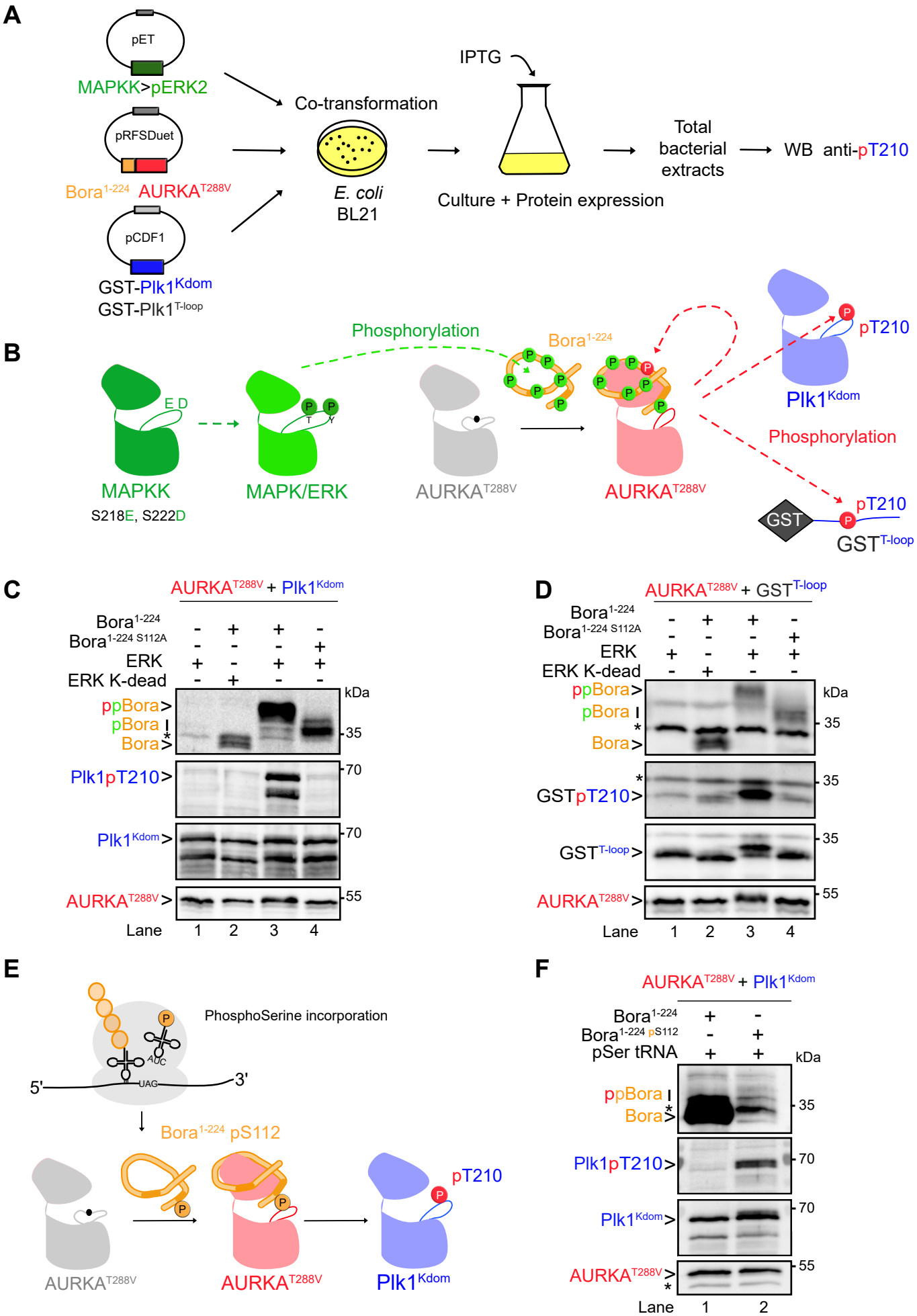

Pillan et al. Figure 4

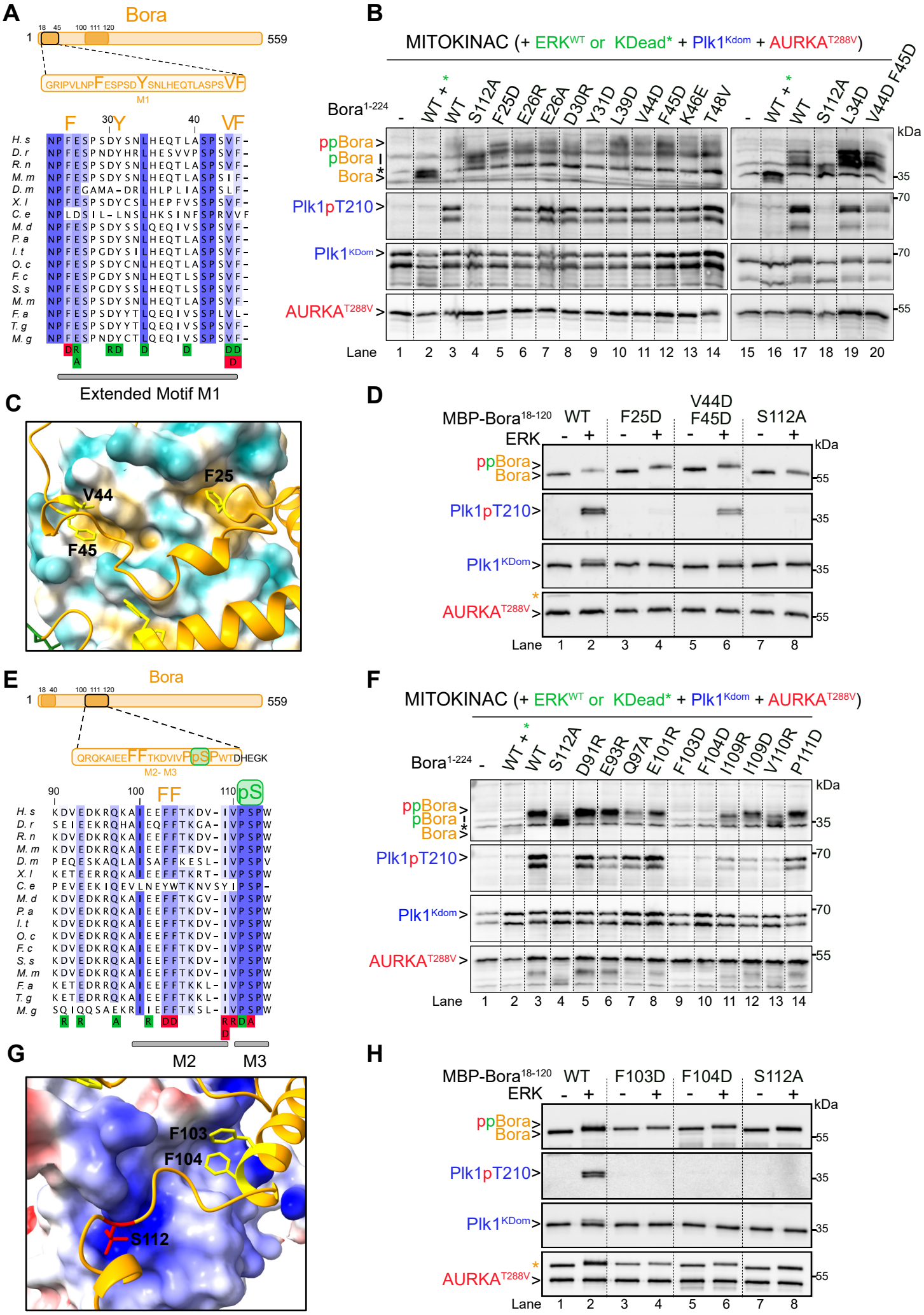

Pillan et al. Figure 5

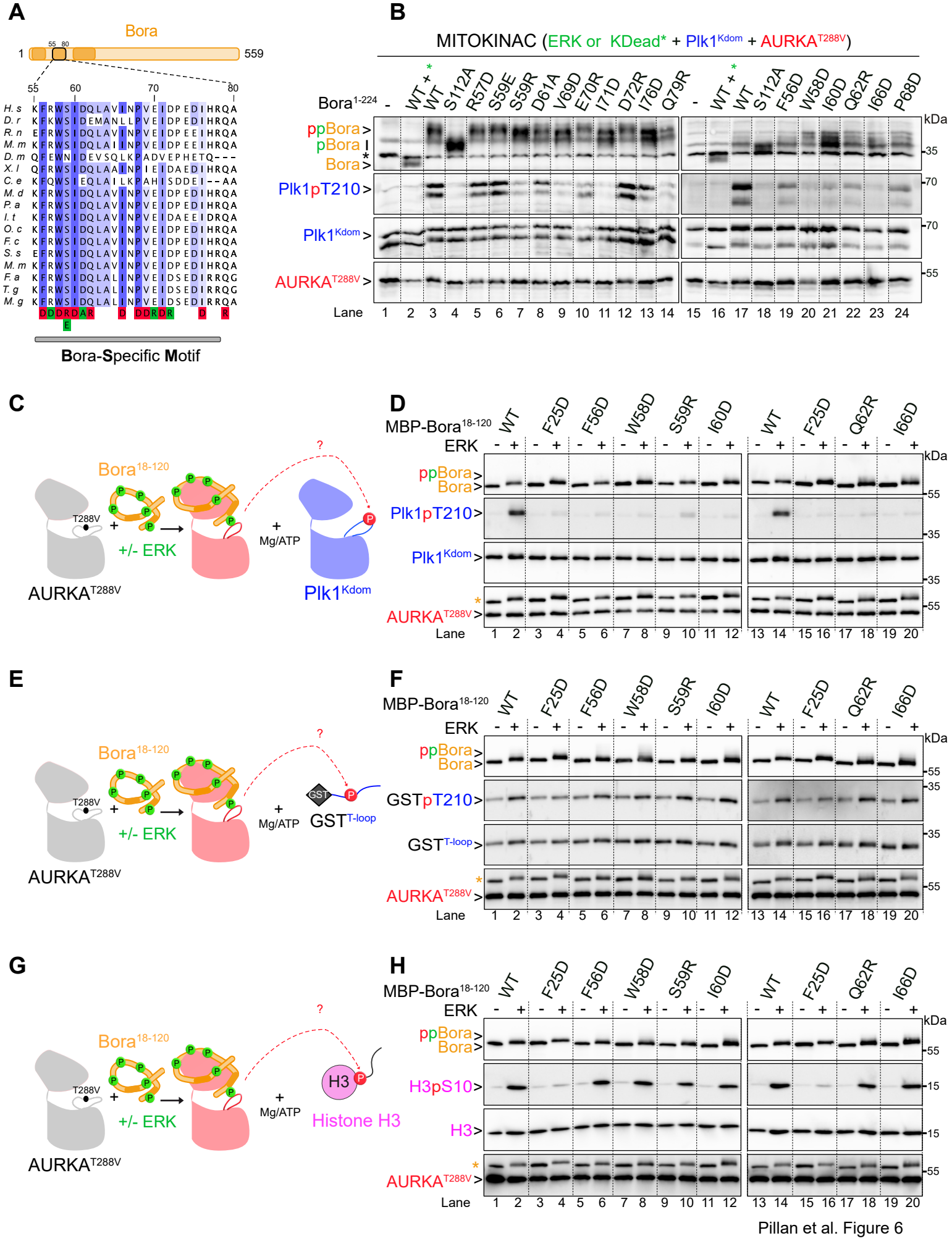

Pillan et al. Figure 6

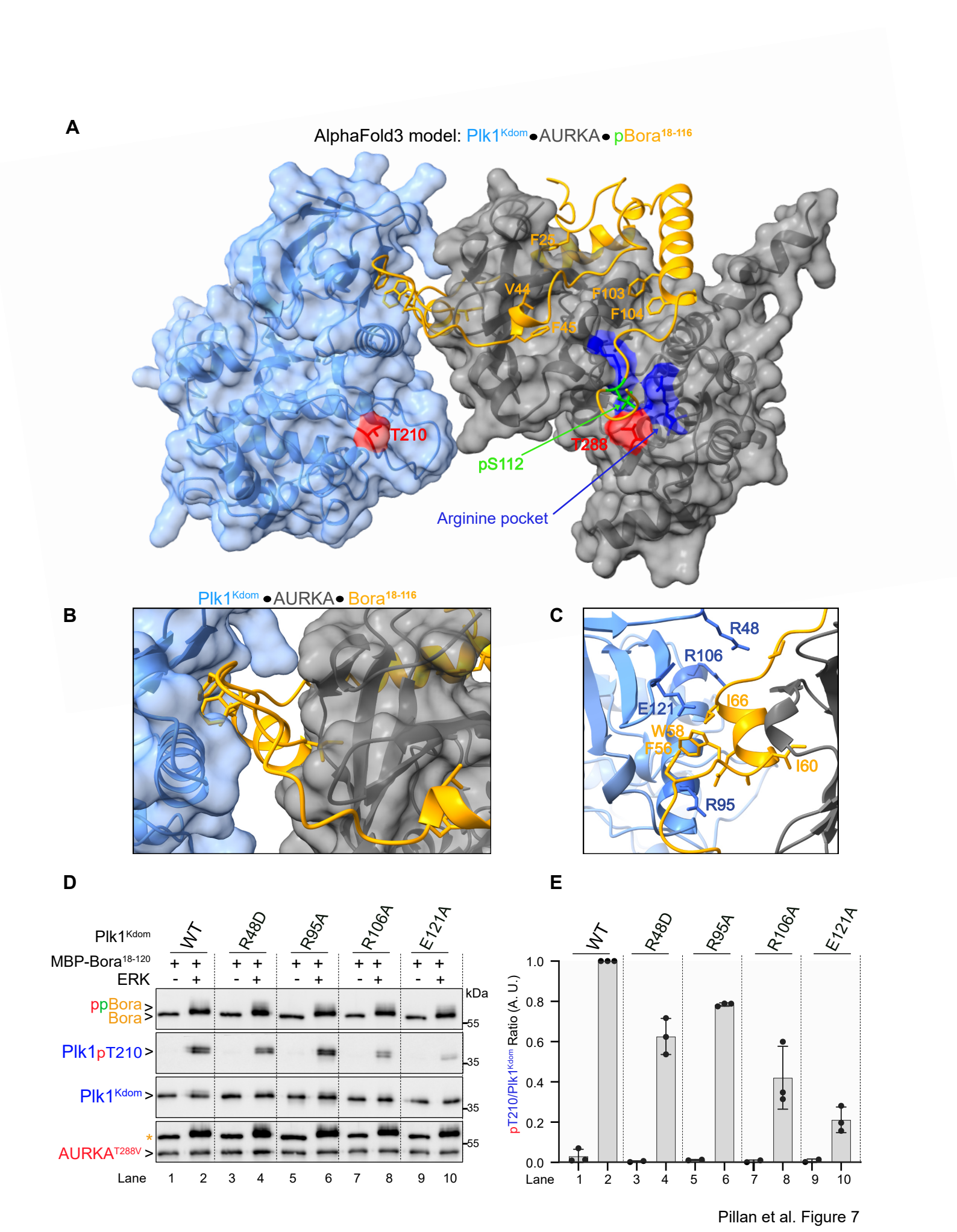

Pillan et al. Figure 7

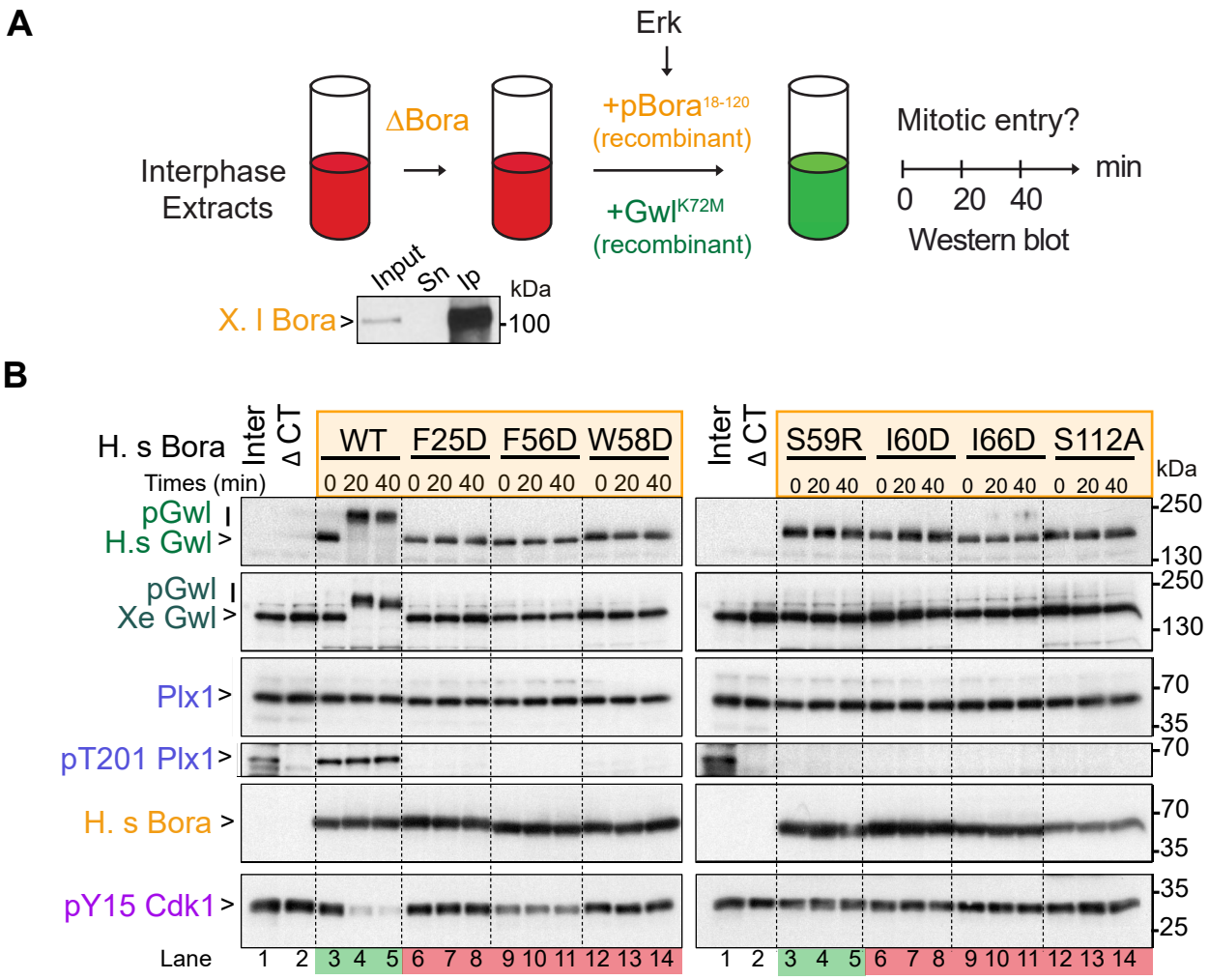

Pillan et al. Figure 8

A

AF3 Bora • AURKA

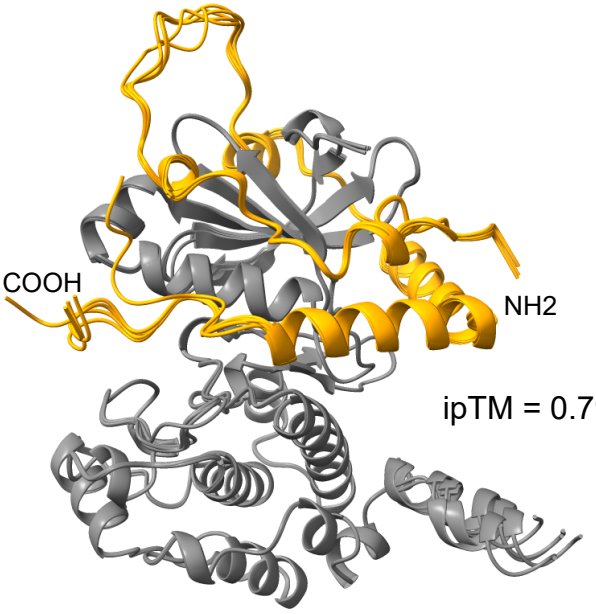

ipTM = 0.79, pTM = 0.84

B

Bora • TACC3

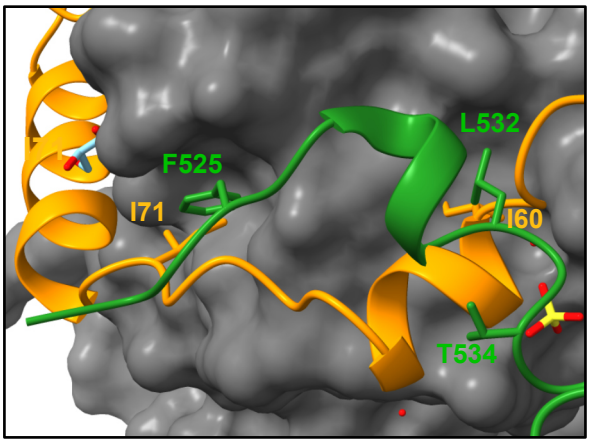

C

Bora • Cep192

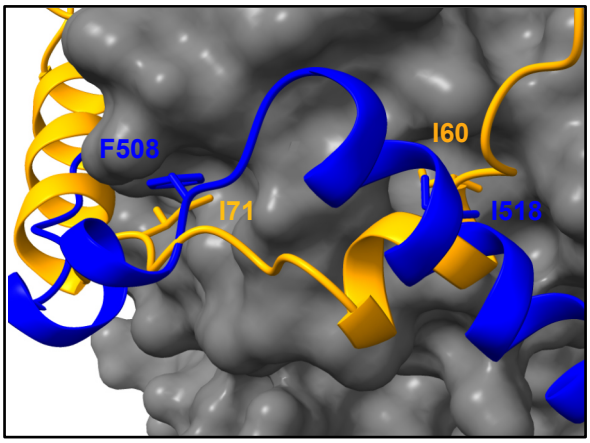

D

AF3 Bora • AURKA

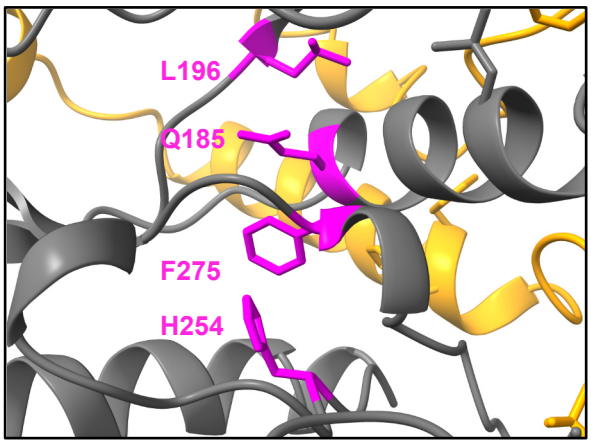

DFG-in R-spine assembled

Pillan et al. Figure S1

A

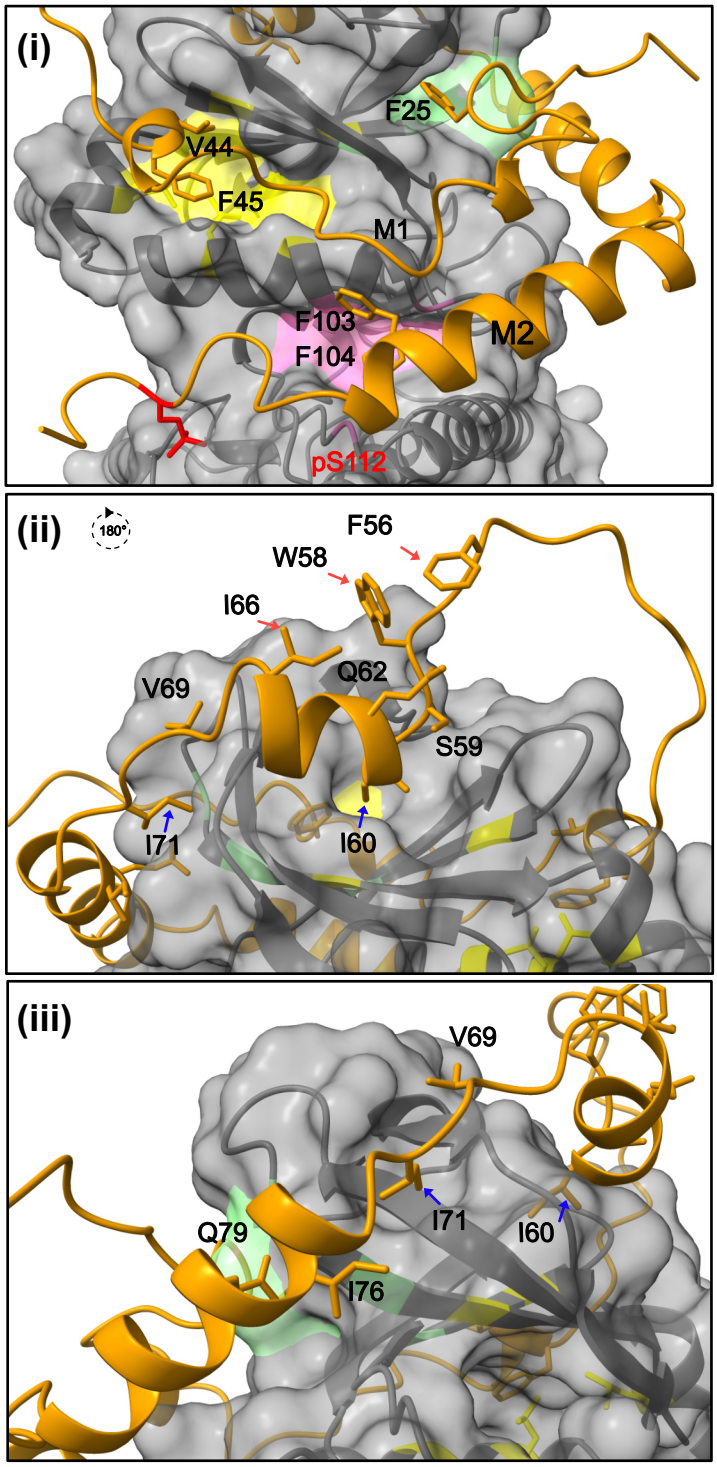

B

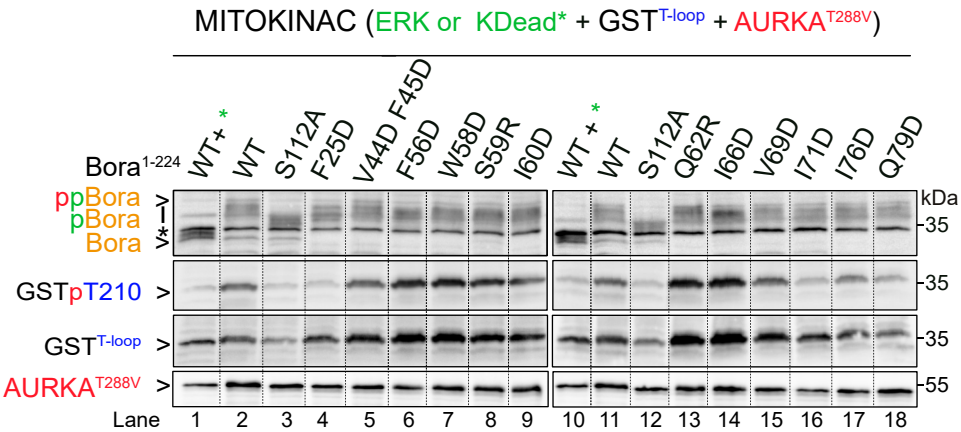

Pillan et al. Figure S2

A

AlfaFold3 model Plk1^{Kdom} • AURKA • Bora$^{18-116}$

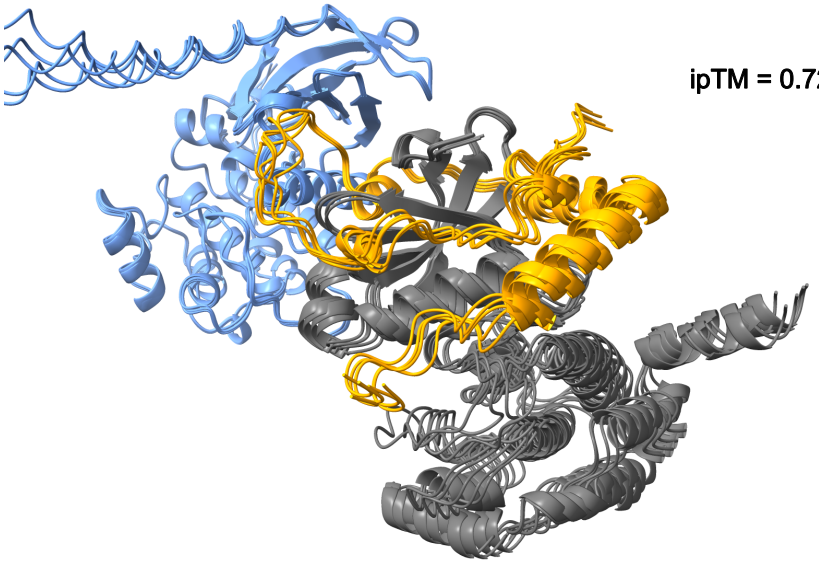

B

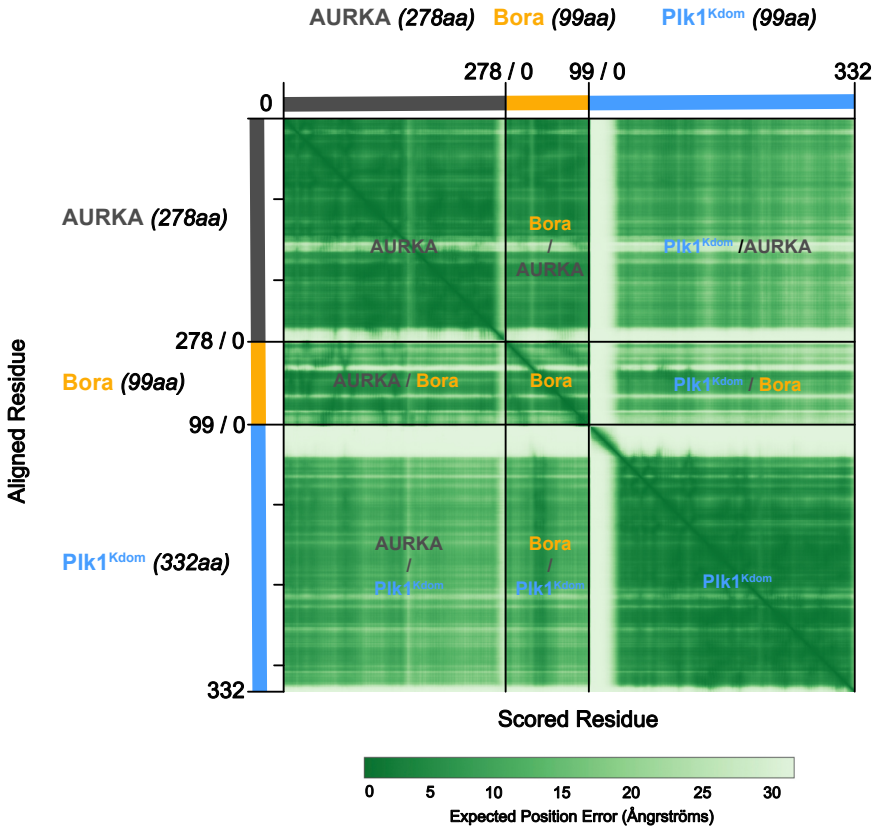

C

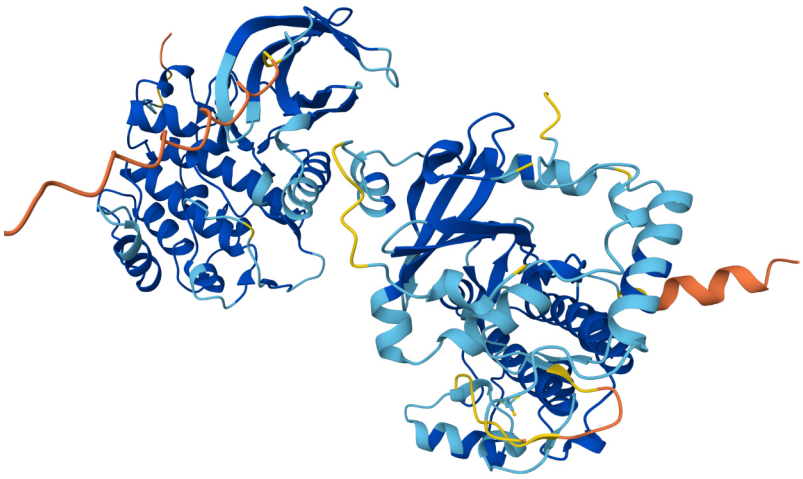

Very high (pLDDT > 90) High (90 > pLDDT > 70) Low (70 > pLDDT > 50) Very low (pLDDT < 50)

Pillan et al. Figure S3